Chemo- and Diastereoselective Tandem Dual Oxidation of B(pin)-substituted Allylic Alcohols: Synthesis of B(pin)-substituted Epoxy Alcohols, 2-Keto-*anti*-1,3-diols and Dihydroxy-tetrahydrofuran-3-ones

Nusrah Hussain, Mahmud M. Hussain, Patrick J. Carroll and Patrick J. Walsh*

P. Roy and Diana T. Vagelos Laboratories, Department of Chemistry, University of Pennsylvania, 231 S. 34th Street, Philadelphia, PA 19104-6323
pwalsh@sas.upenn.edu

Supporting Information

Part 2

Table of Contents Page **Page**

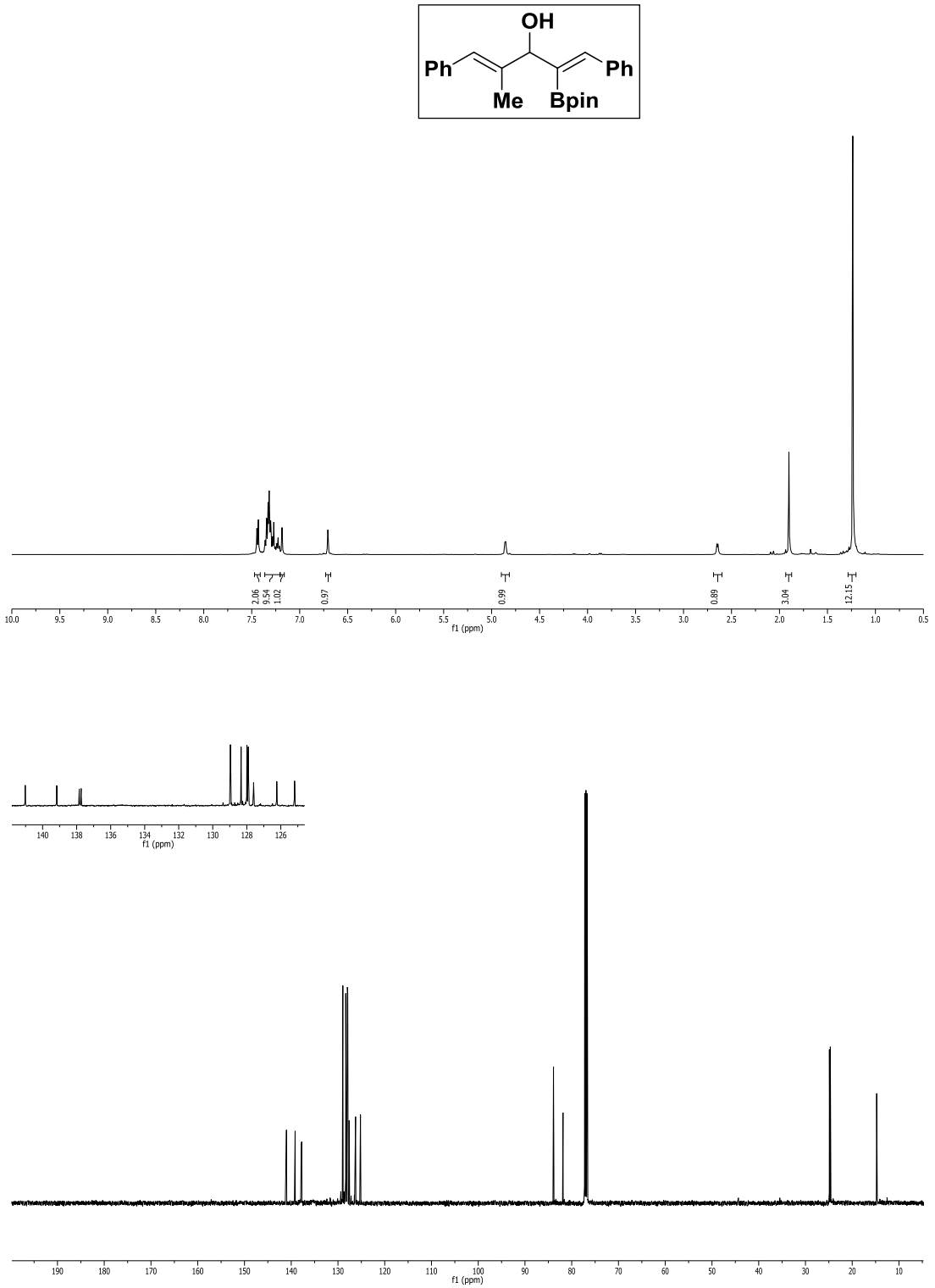

Figure S1 (1k). 300 MHz ^{1}H and 125 MHz $^{13}C\{^{1}H\}$ NMR of (1*E*,4*E*)-2-methyl-1,5-diphenyl-4(4,4,5,5-tetramethyl-1,3,2-dioxaborolane-2-yl)penta-1,4-dien-3-ol in $CDCl_3$.

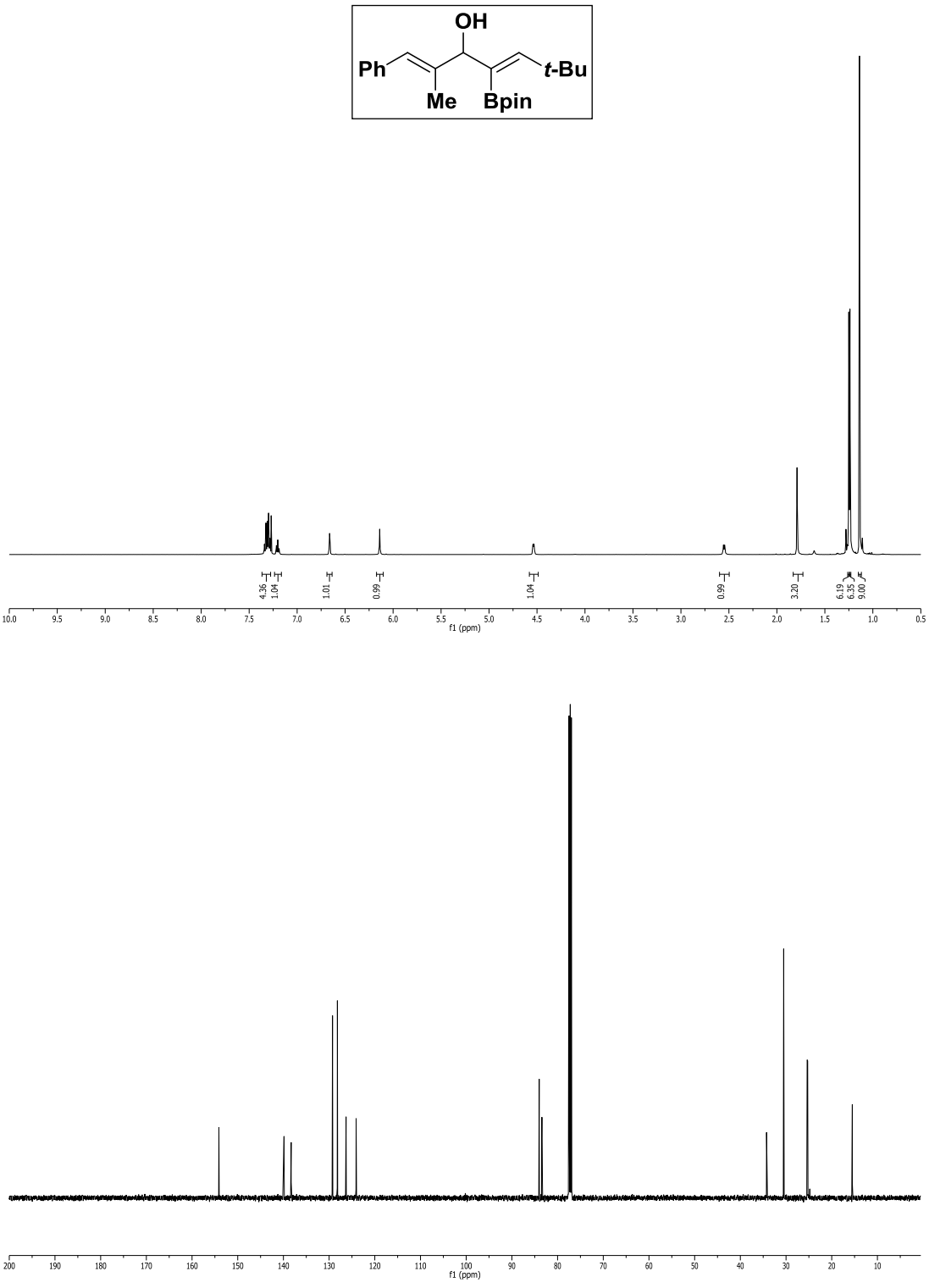

Figure S2 (1l). 500 MHz ^{1}H and 125 MHz ^{13}C{^{1}H} NMR of (1*E*,4*E*)-2,6,6-trimethyl-1-phenyl-4-(4,4,5,5-tetramethyl-1,3,2-dioxaborolan-2-yl)hepta-1,4-dien-3-ol in $CDCl_3$.

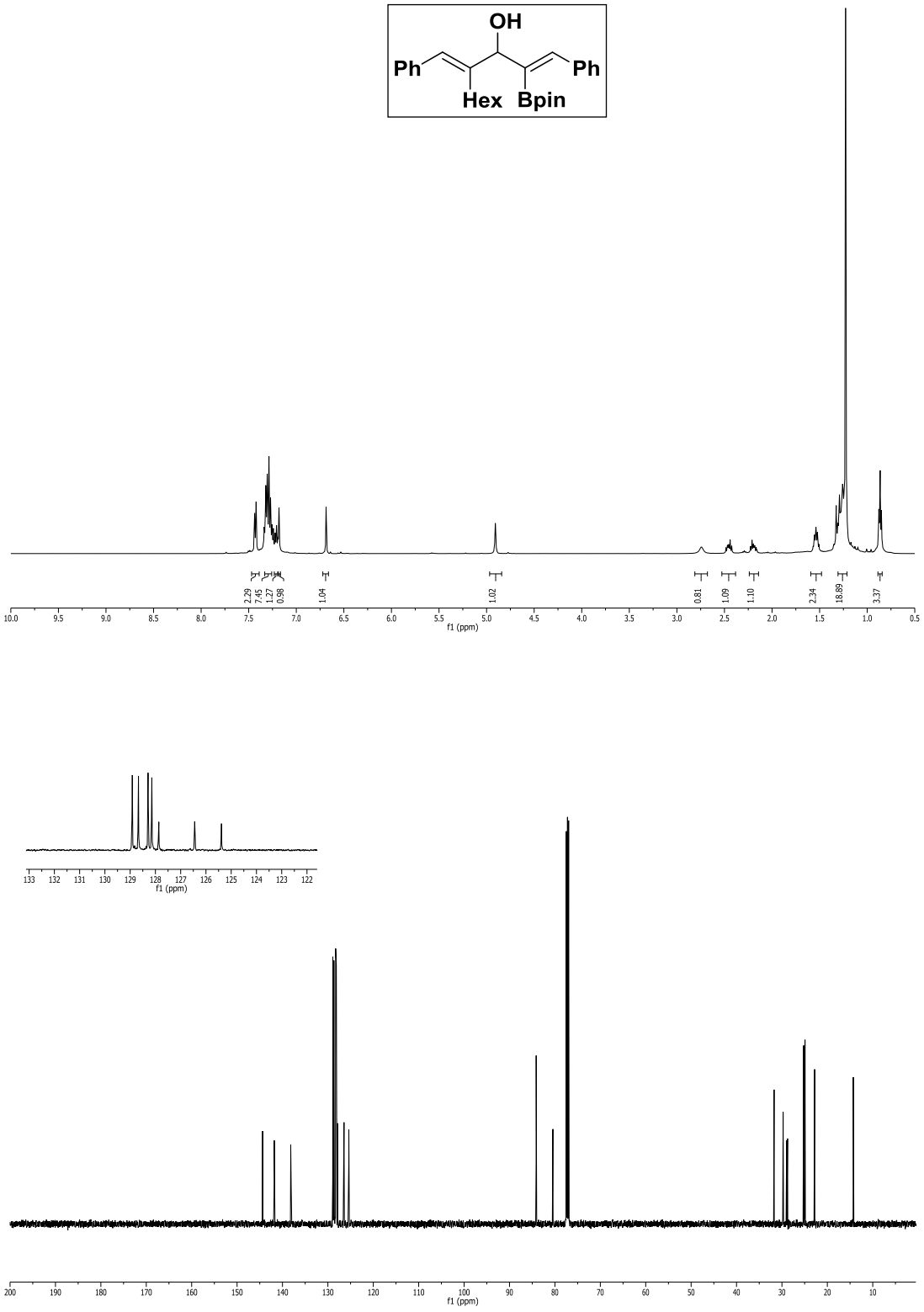

Figure S3 (1m). 500 MHz ^{1}H and 125 MHz ^{13}C{^{1}H} NMR of (1*E*,4*E*)-4-benzylidene-1-phenyl-2-(4,4,5,5-tetramethyl-1,3,2-dioxaborolan-2-yl)dec-1-en-3-ol in $CDCl_3$.

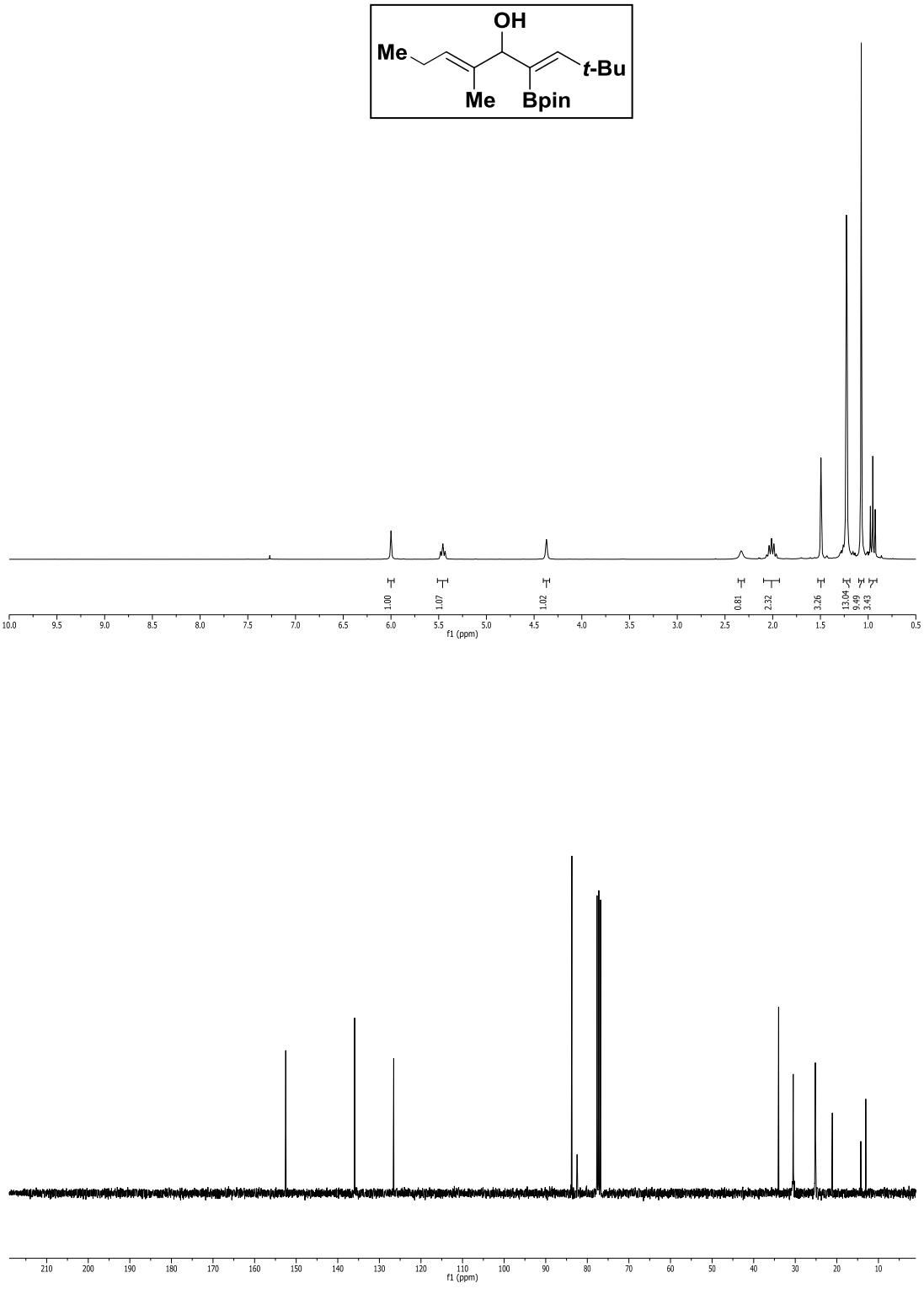

Figure S4 (1n). 500 MHz ^{1}H and 125 MHz $^{13}C\{^{1}H\}$ NMR of (3*E*,6*E*)-2,2,6-trimethyl-4-(4,4,5,5-tetramethyl-1,3,2-dioxaborolan-2-yl)nona-3,6-dien-5-ol in $CDCl_3$.

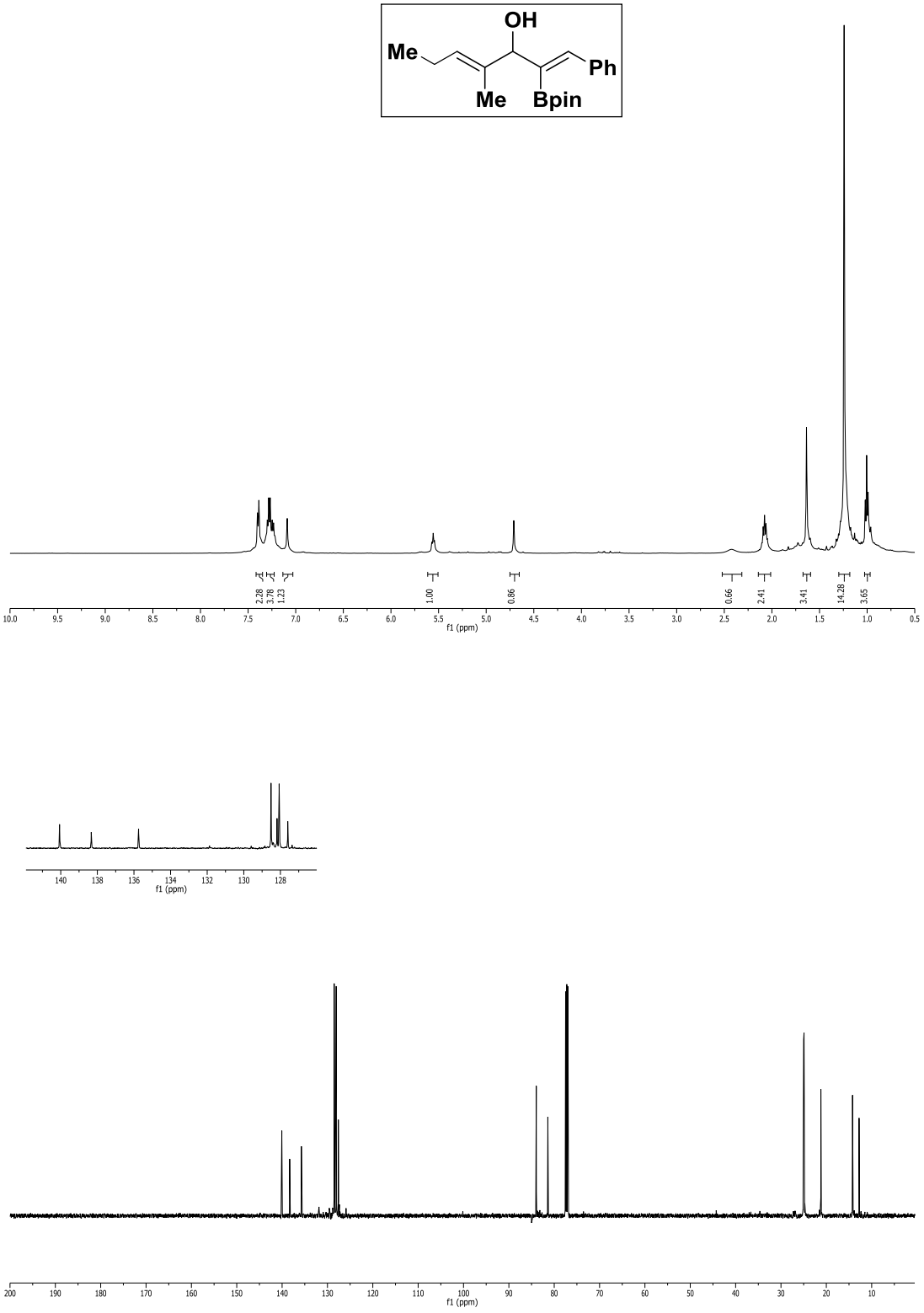

Figure S5 (1o). 500 MHz ^{1}H and 125 MHz ^{13}C{^{1}H} NMR of (1*E*,4*E*)-4-methyl-1-phenyl-2-(4,4,5,5-tetramethyl-1,3,2-dioxaborolan-2-yl)hepta-1,4-dien-3-ol in $CDCl_3$.

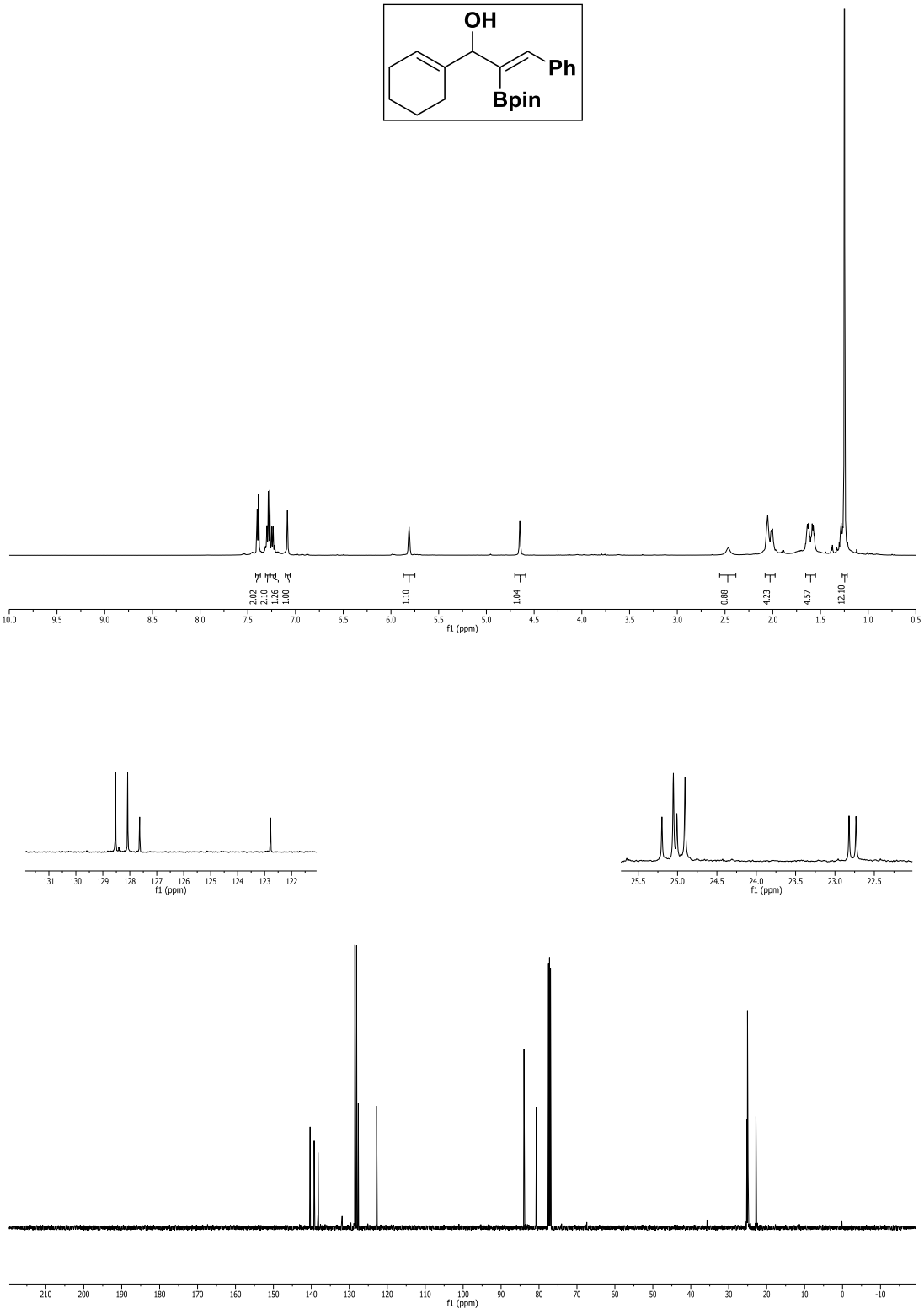

Figure S6 (1p). 500 MHz ^{1}H and 125 MHz $^{13}C\{^{1}H\}$ NMR of **(***E***)**-1-cyclohexenyl-3-phenyl-2-(4,4,5,5-tetramethyl-1,3,2-dioxaborolan-2-yl)prop-2-en-1-ol in $CDCl_3$.

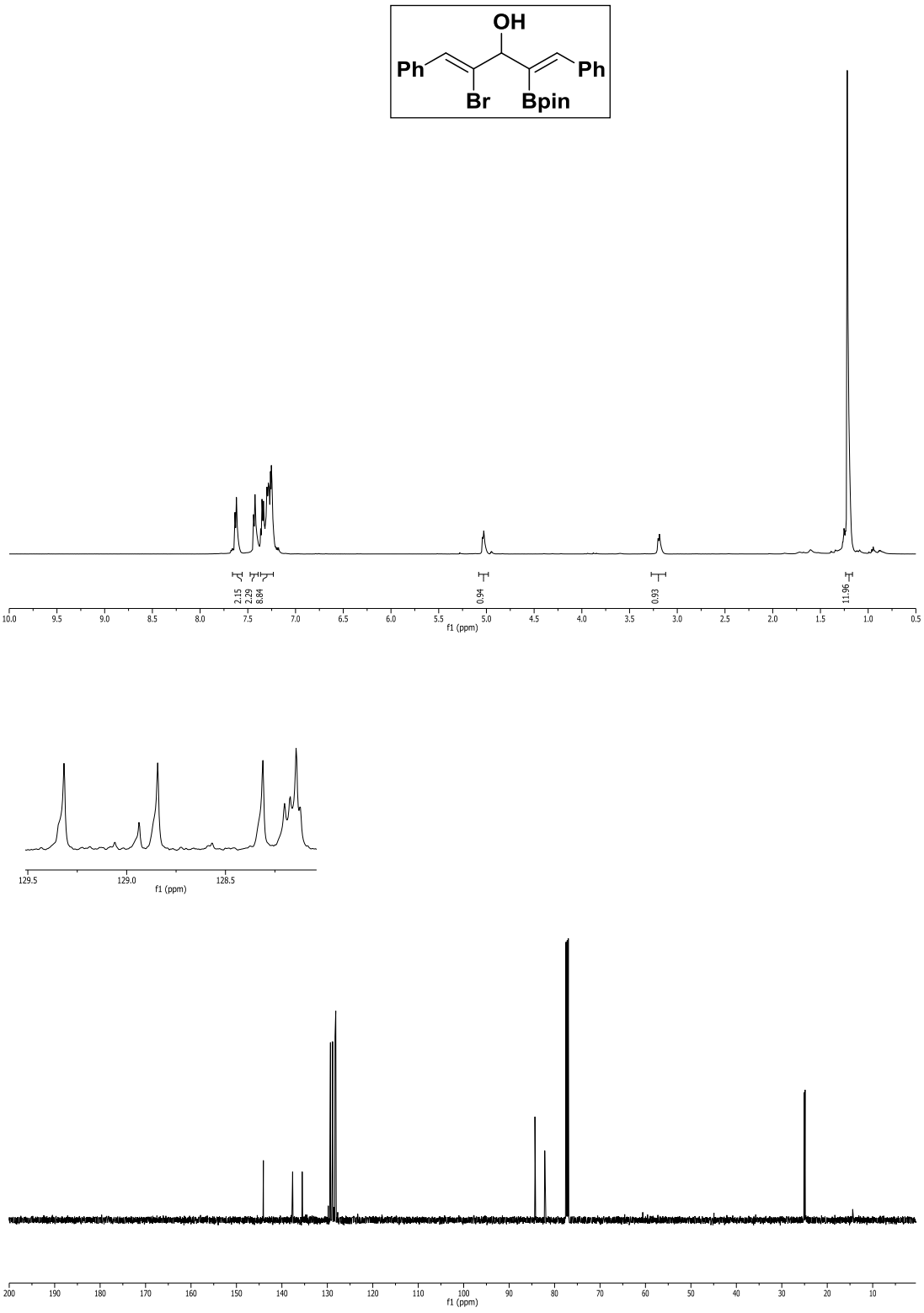

Figure S7 (1q). 500 MHz ^{1}H and 125 MHz ^{13}C{^{1}H} NMR of (1*Z*,4*E*)-2-bromo-1,5-diphenyl-4-(4,4,5,5-tetramethyl-1,3,2-dioxaborolan-2-yl)penta-1,4-dien-3-ol in $CDCl_3$.

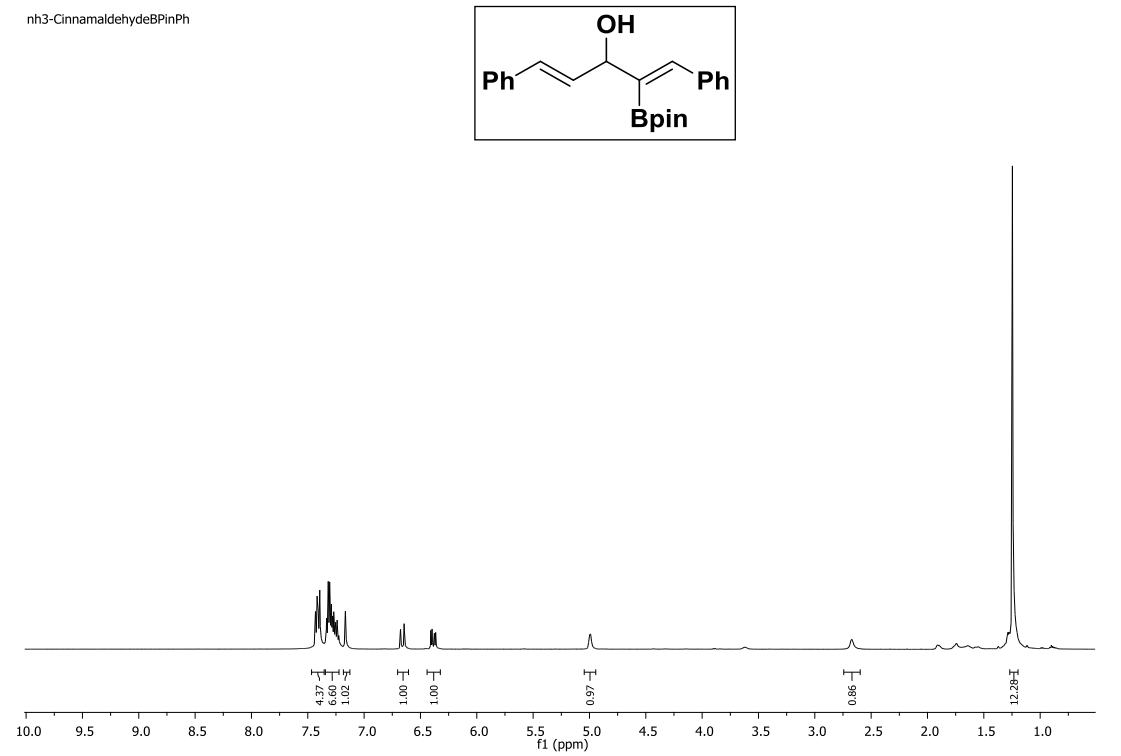

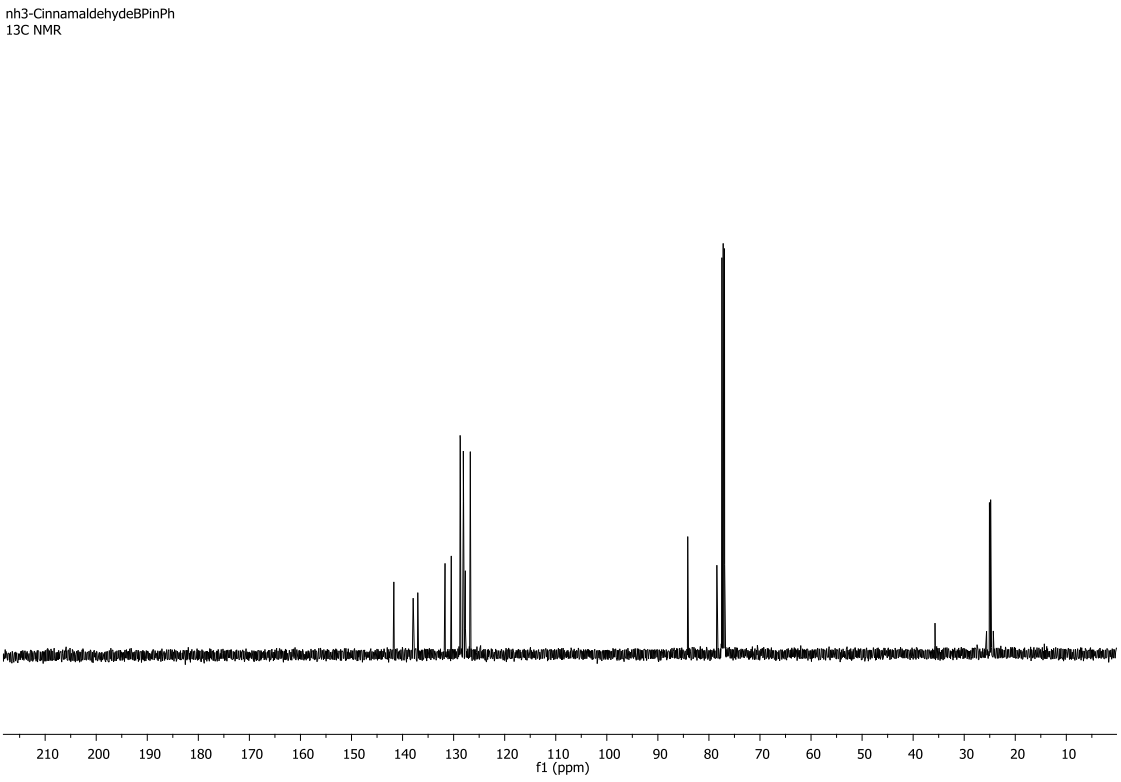

Figure S8 (1r). 500 MHz ^{1}H and 125 MHz ^{13}C{^{1}H} NMR of (1*E*,4*E*)-1,5-diphenyl-2-(4,4,5,5-tetramethyl-1,3,2-dioxaborolan-2-yl)penta-1,4-dien-3-ol in $CDCl_3$.

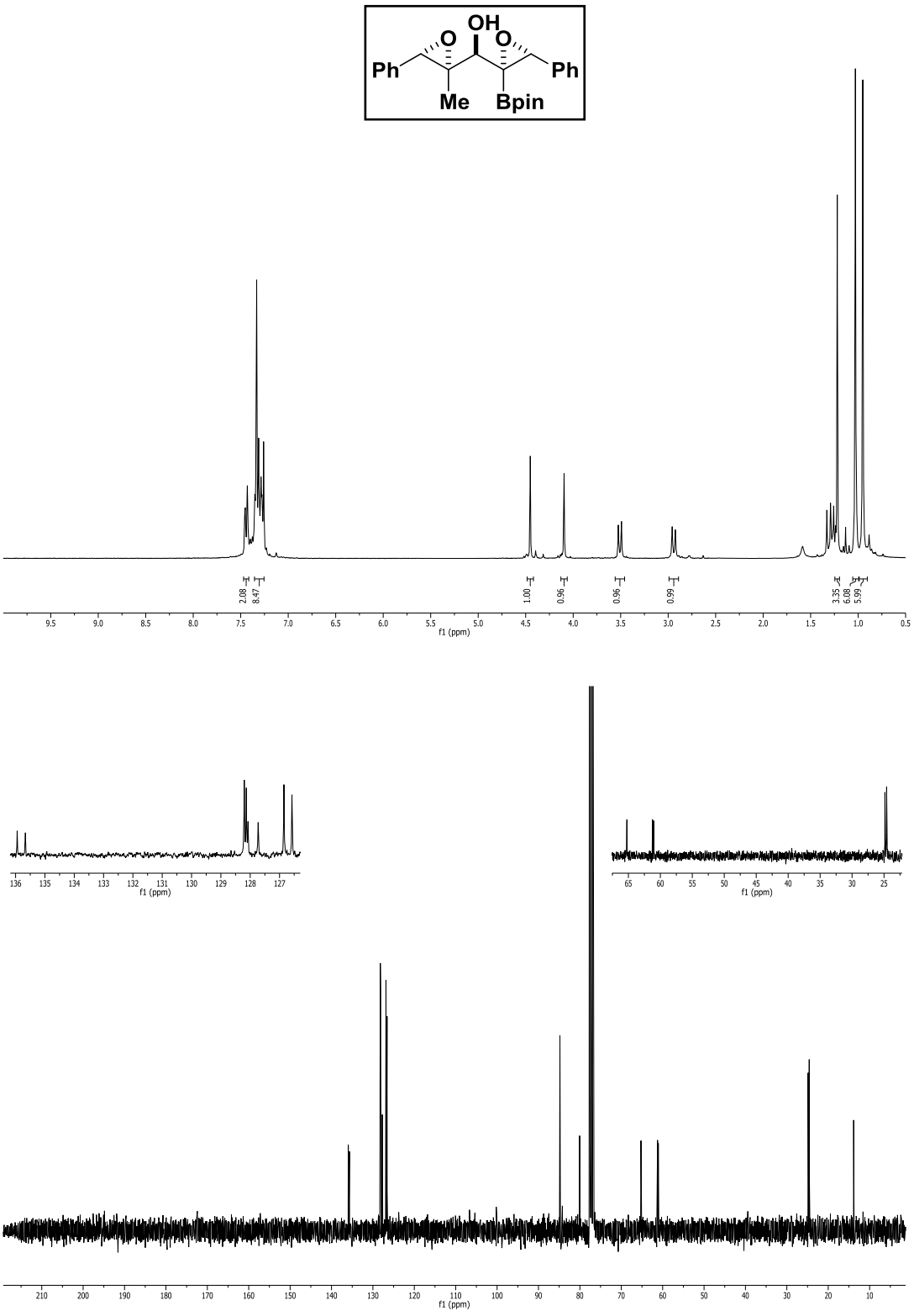

Figure S9 (2k). 500 MHz ^{1}H and 125 MHz $^{13}C\{^{1}H\}$ NMR of (2-methyl-3-phenyloxiran-2-yl)(3-phenyl-2-(4,4,5,5-tetramethyl-1,3,2-dioxaborolan-2-yl)methanol in $CDCl_3$.

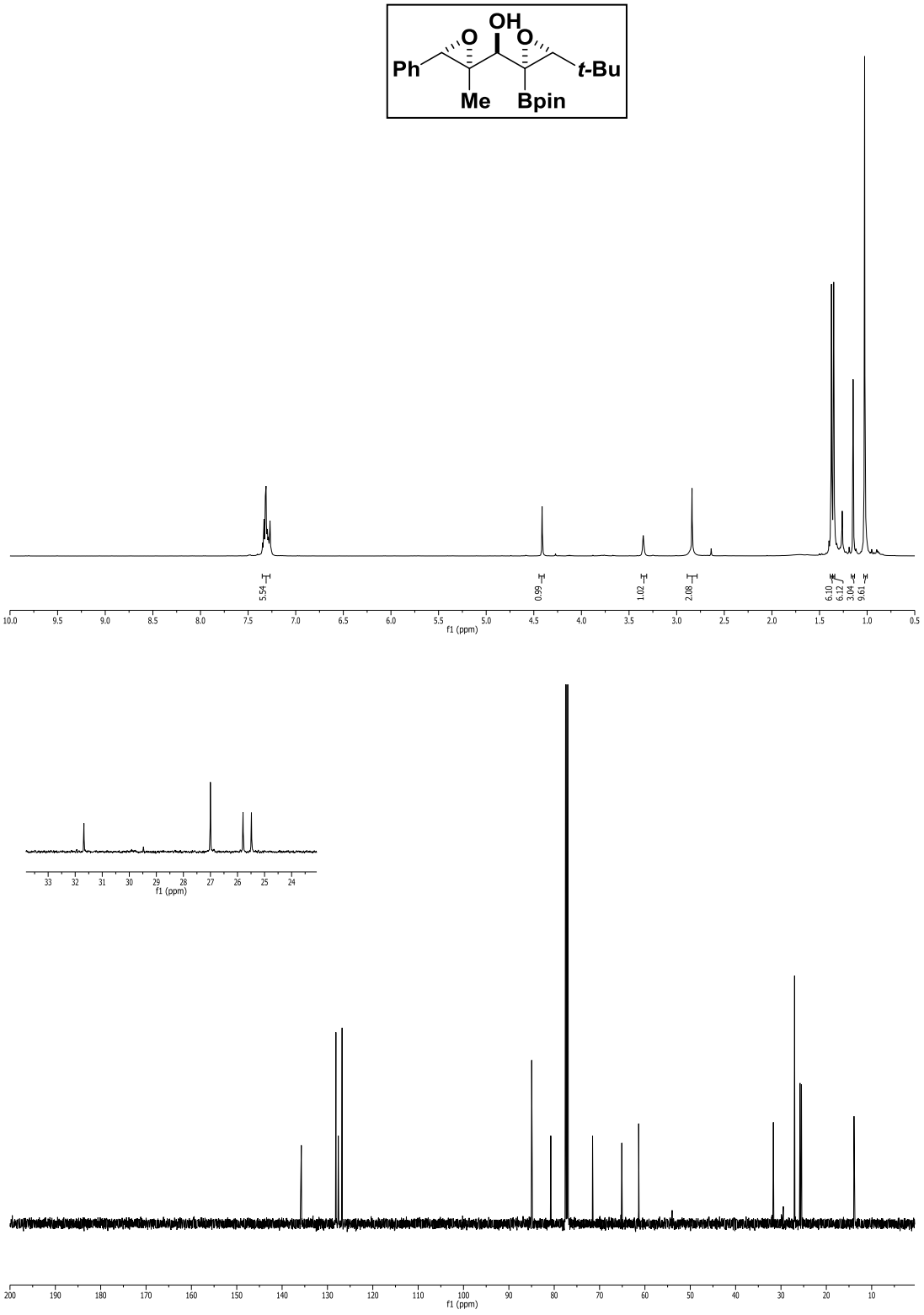

Figure S10 (2l). 500 MHz ^{1}H and 125 MHz $^{13}C\{^{1}H\}$ NMR of (3-*tert*-butyl-2-(4,4,5,5-tetramethyl-1,3,2-dioxaborolan-2-yl)(2-methyl-3-phenyloxiran-2-yl)methanol in $CDCl_3$.

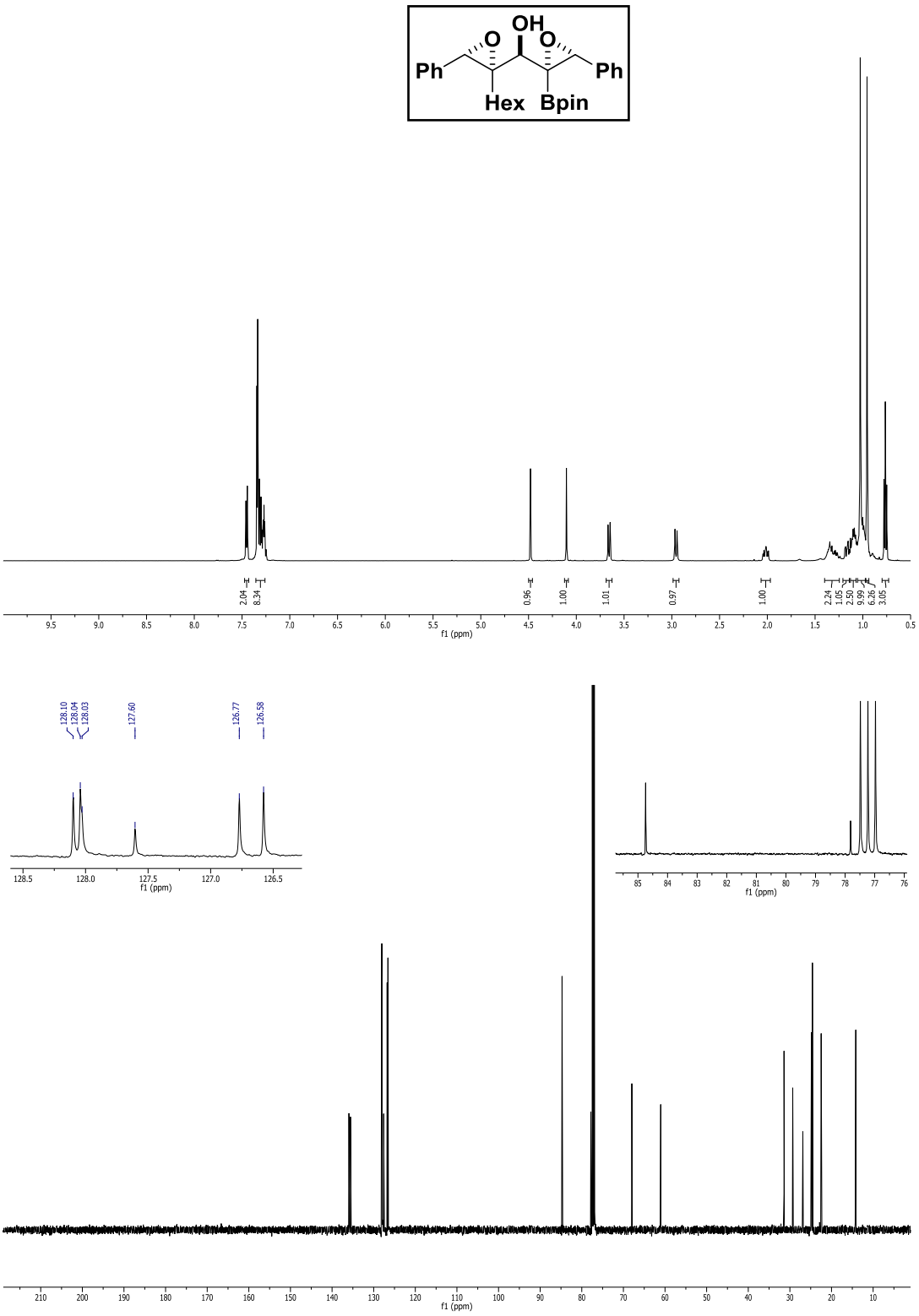

Figure S11 (2m). 500 MHz ^{1}H and 125 MHz $^{13}C\{^{1}H\}$ NMR of (2-hexyl-3-phenyloxiran-2-yl)(3-phenyl-2-(4,4,5,5-tetramethyl-1,3,2-dioxaborolan-2-yl)oxiran-2-yl)methanol in $CDCl_3$.

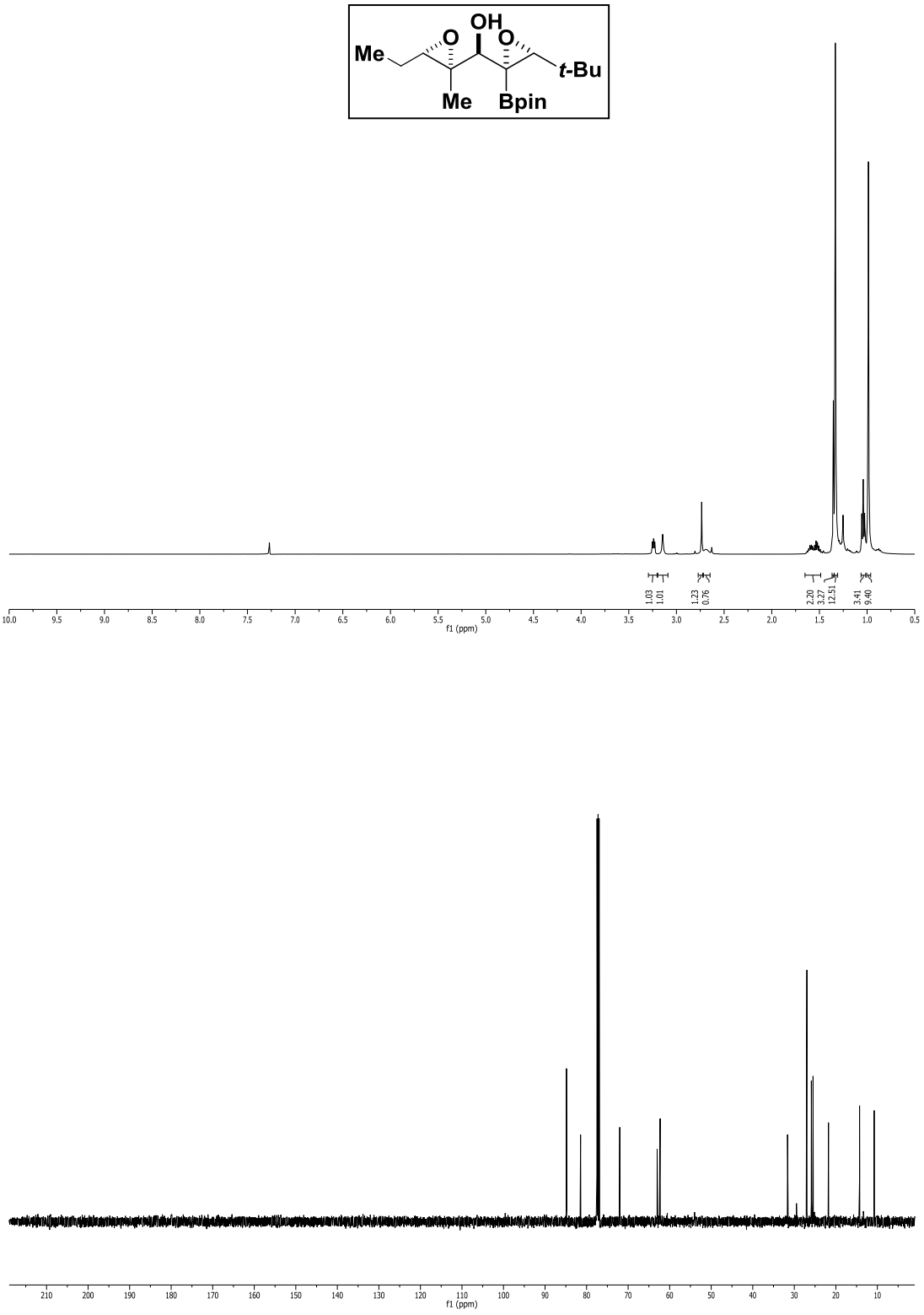

Figure S12 (2n). 500 MHz ^{1}H and 125 MHz ^{13}C{^{1}H NMR (3-(*tert*-butyl)-2-(4,4,5,5-tetramethyl-1,3,2-dioxaborolan-2-yl)oxiran-2-yl)(3-ethyl-2-methyloxiran-2-yl)methanol in $CDCl_3$.

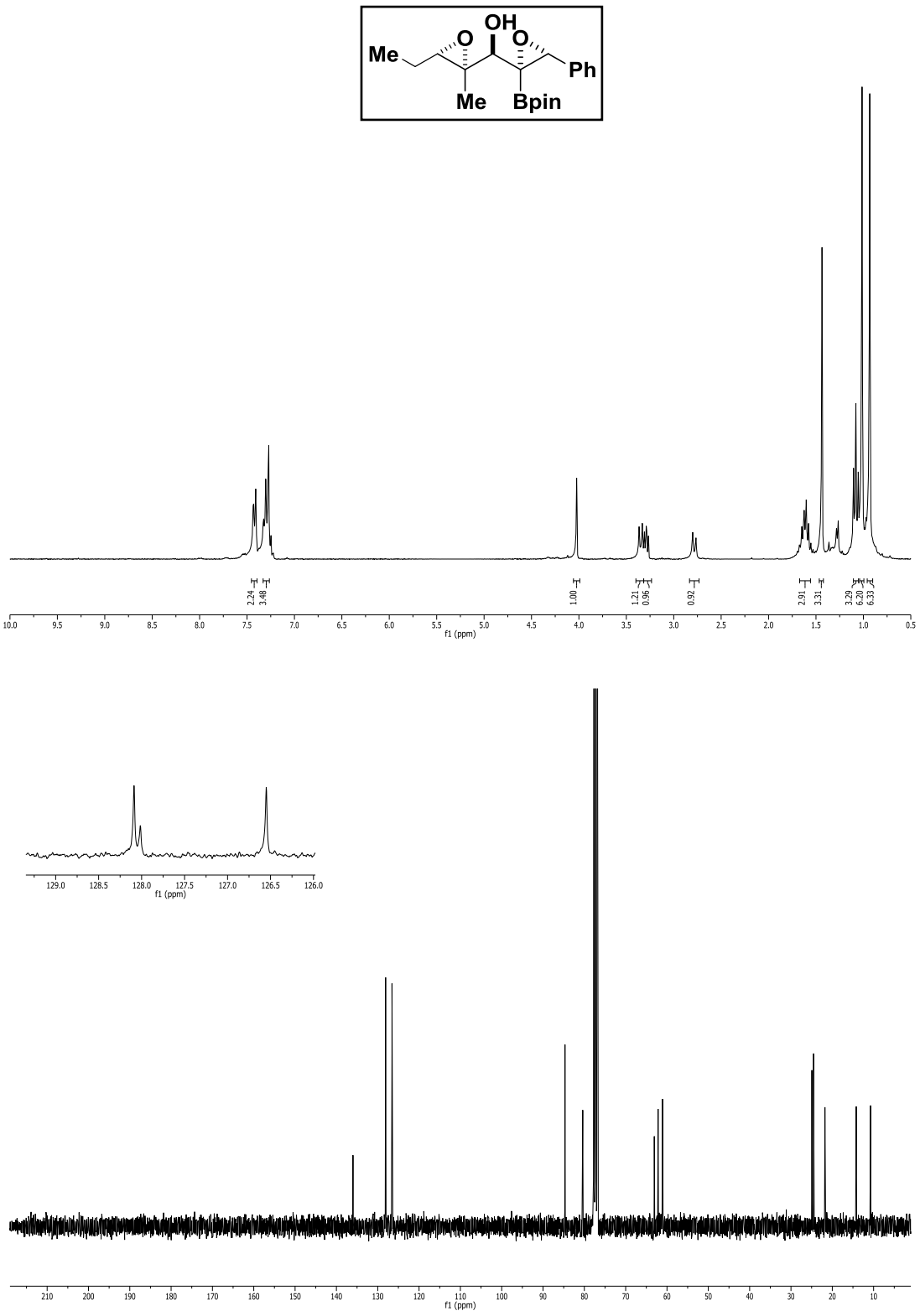

Figure S13 (2o). 500 MHz ^{1}H and 125 MHz $^{13}C\{^{1}H\}$ NMR of (3-ethyl-2-methyl-2-methyloxiran-2-yl)(3-phenyl-2-(4,4,5,5-tetramethyl-1,3,2-dioxaborolan-2-yl)methanol in $CDCl_3$.

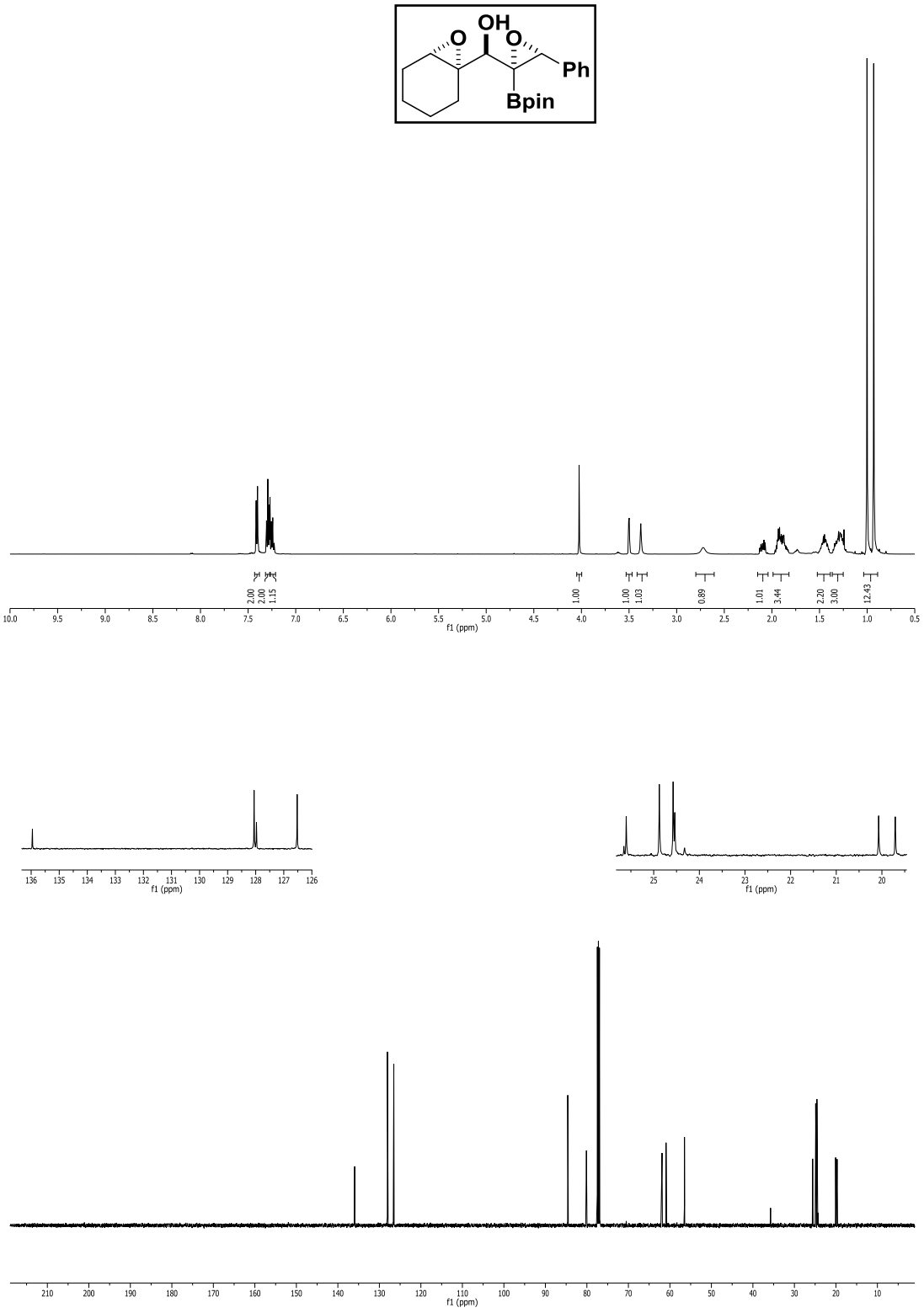

Figure S14 (2p). 500 MHz ^{1}H and 125 MHz $^{13}C\{^{1}H\}$ NMR of (7-oxabicycloheptan-1-yl)(3-phenyl-2-(4,4,5,5-tetramethyl-1,3,2-dioxaborolan-2-yl)oxiran-2-yl)methanol in $CDCl_3$.

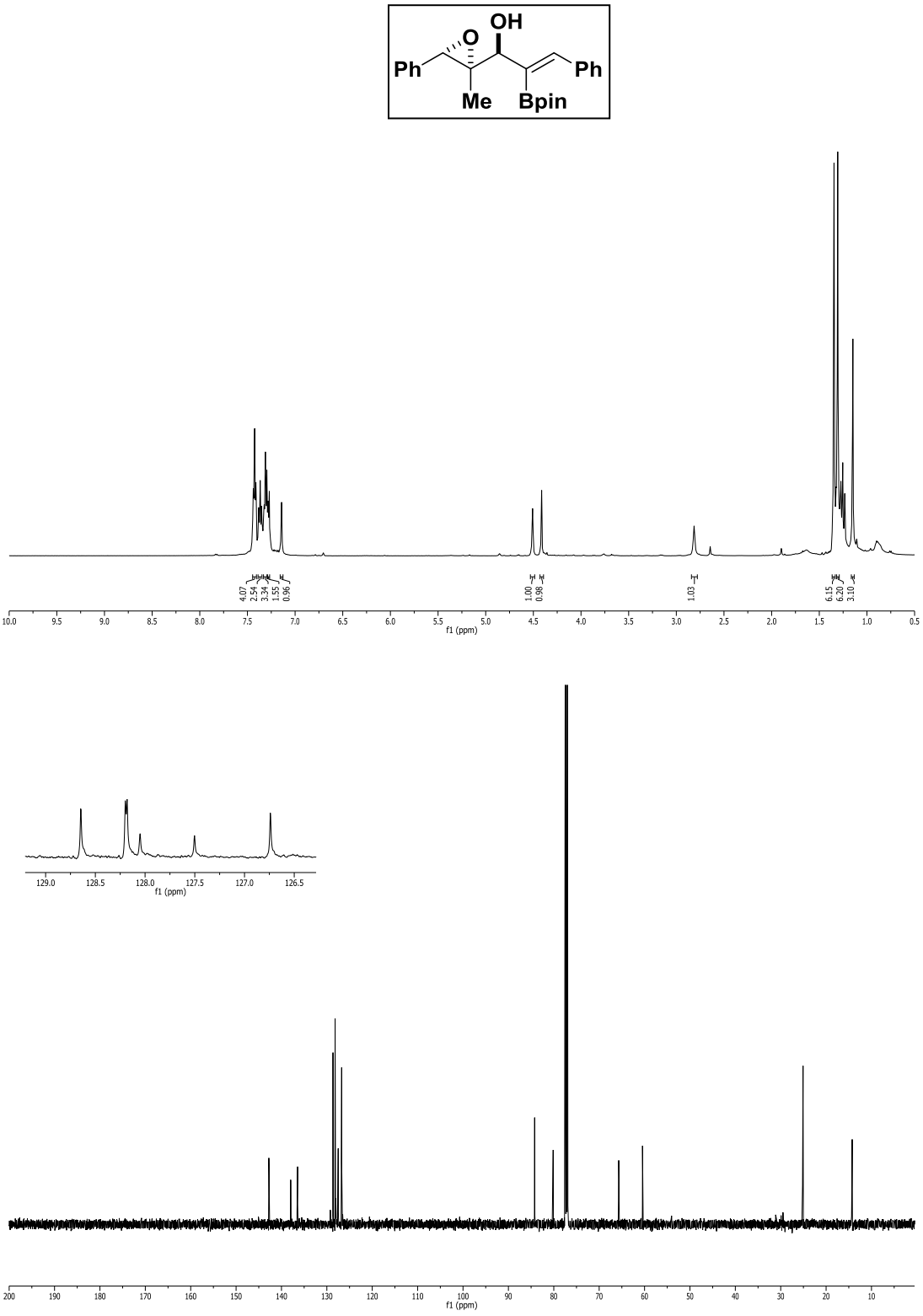

Figure S15 (3k). 500 MHz ^{1}H and 125 MHz $^{13}C\{^{1}H\}$ NMR of (*E*)-1-(2-methyl-3-phenyloxiran-2-yl)-3-phenyl-2-(4,4,5,5-tetramethyl-1,3,2-dioxaborolan-2-yl)prop-2-en-1-ol in $CDCl_3$.

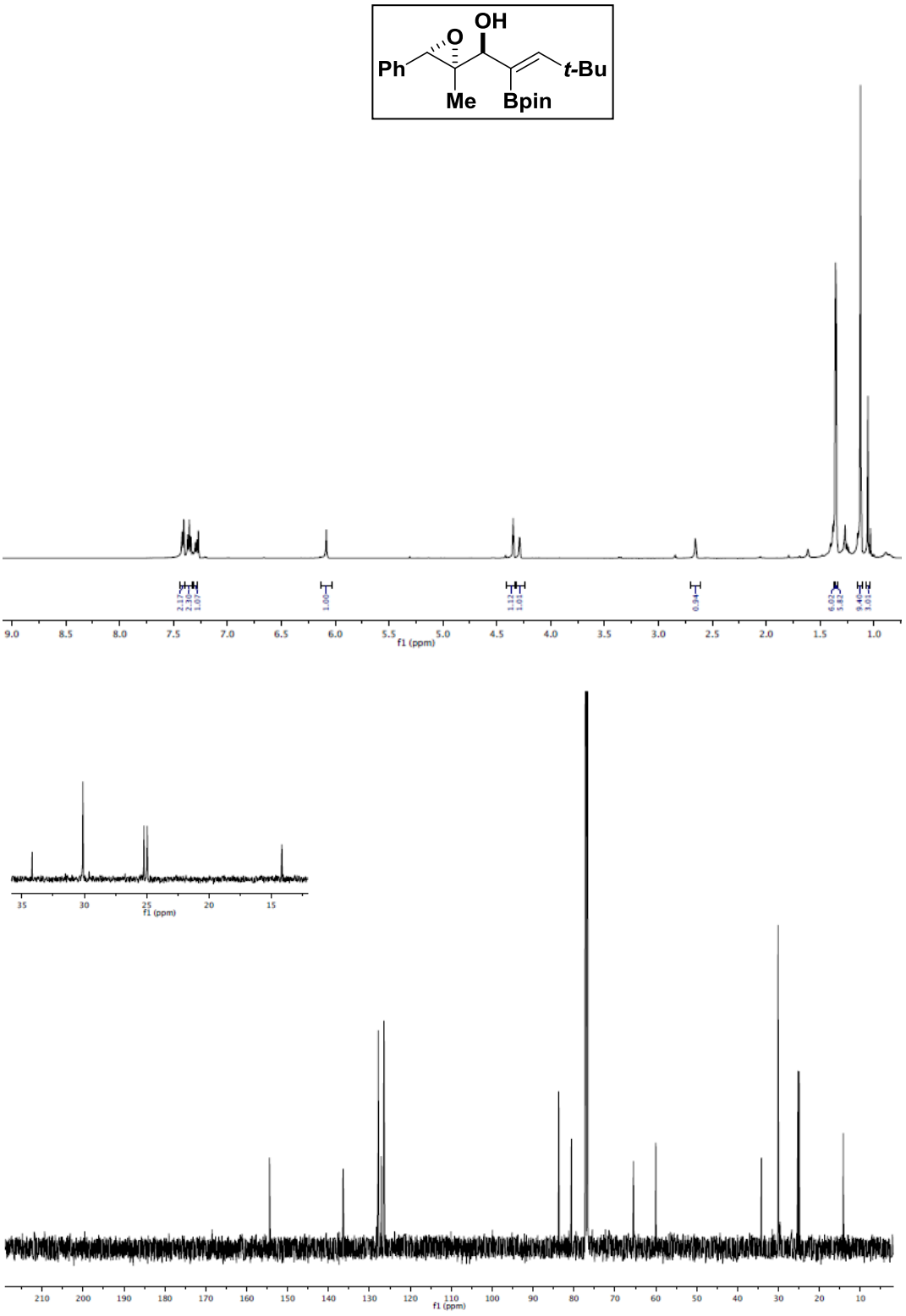

Figure S16 (3l). 500 MHz ^{1}H and 125 MHz ^{13}C{^{1}H} NMR of (*E*)-4,4-dimethyl-1-(2-methyl-3-phenyloxiran-2-yl)-2-(4,4,5,5-tetramethyl-1,3,2-dioxaborolan-2-yl)pent-2-en-1-ol in $CDCl_3$.

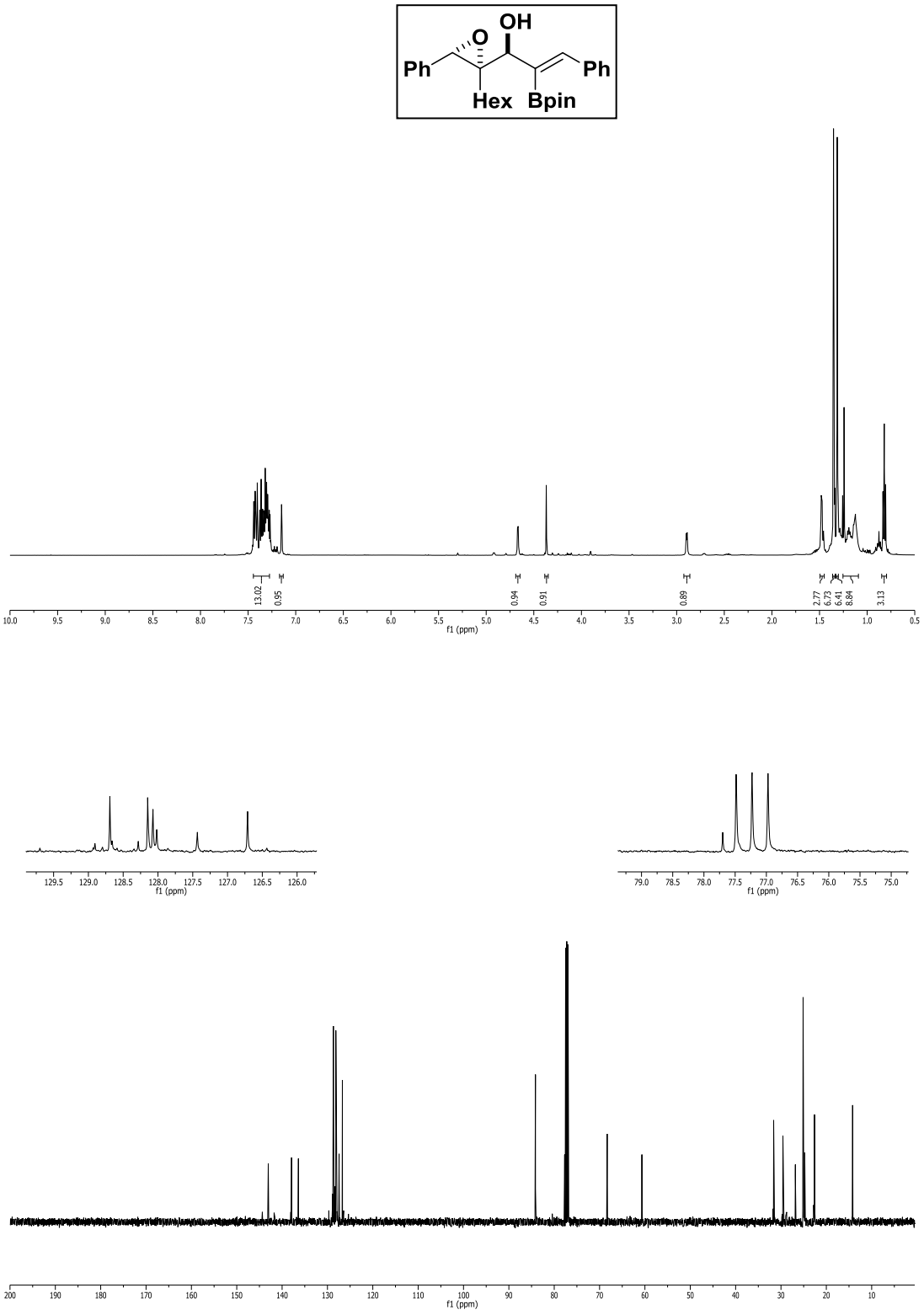

Figure S17 (3m). 500 MHz ^{1}H and 125 MHz ^{13}C{^{1}H} NMR of (*E*)-1-(2-hexyl-3-phenyloxiran-2-yl)-3-phenyl-2-(4,4,5,5-tetramethyl-1,3,2-dioxaborolan-2-yl)prop-2-en-1-ol in $CDCl_3$.

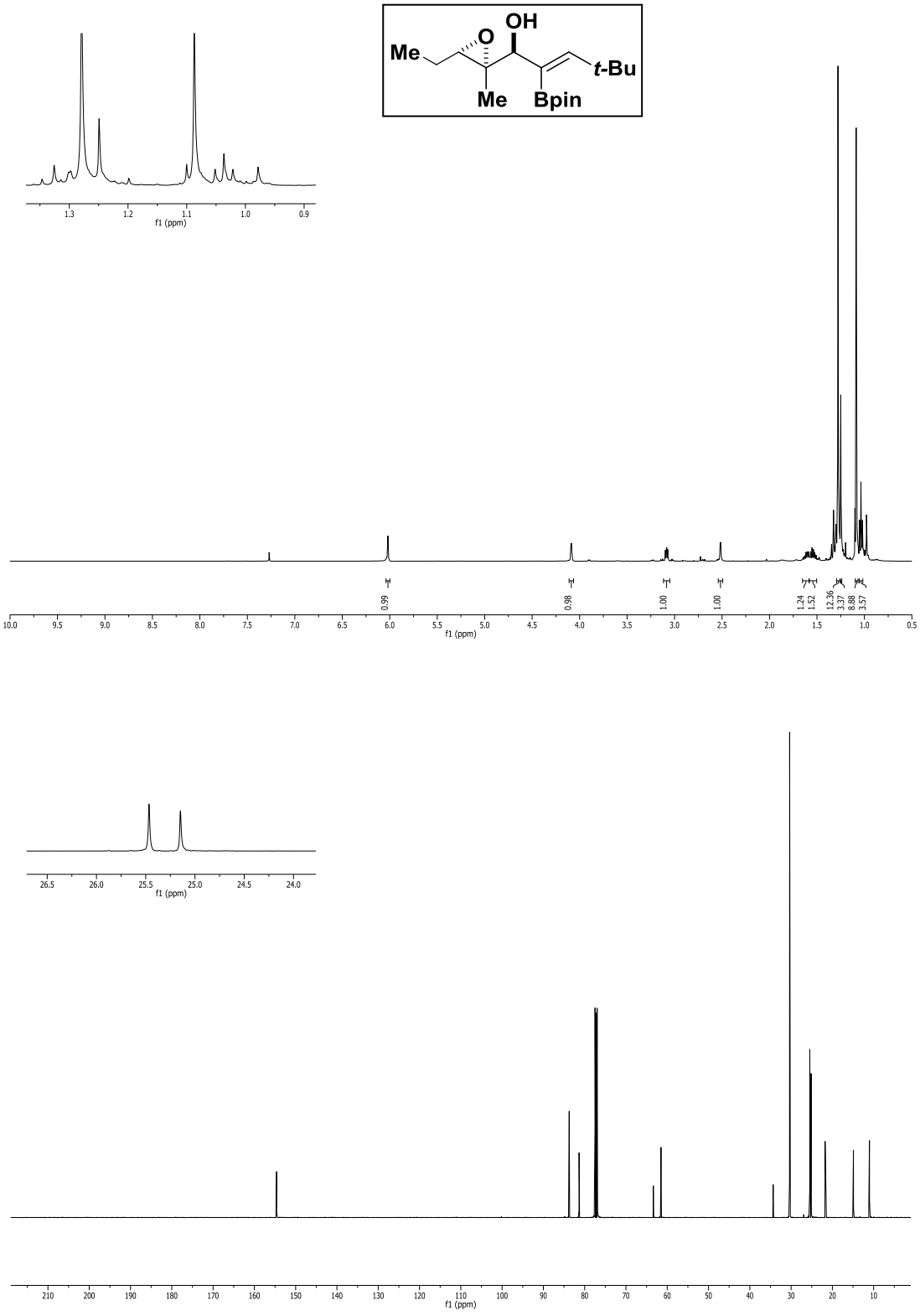

Figure S18 (3n). 500 MHz ^{1}H and 125 MHz ^{13}C{^{1}H} NMR of (*E*)-1-(3-ethyl-2-methyloxiran-2-yl)-4,4--dimethyl-2-(4,4,5,5-tetramethyl-1,3,2-dioxaborolan-2-yl)pent-2-en-1-ol in $CDCl_3$.

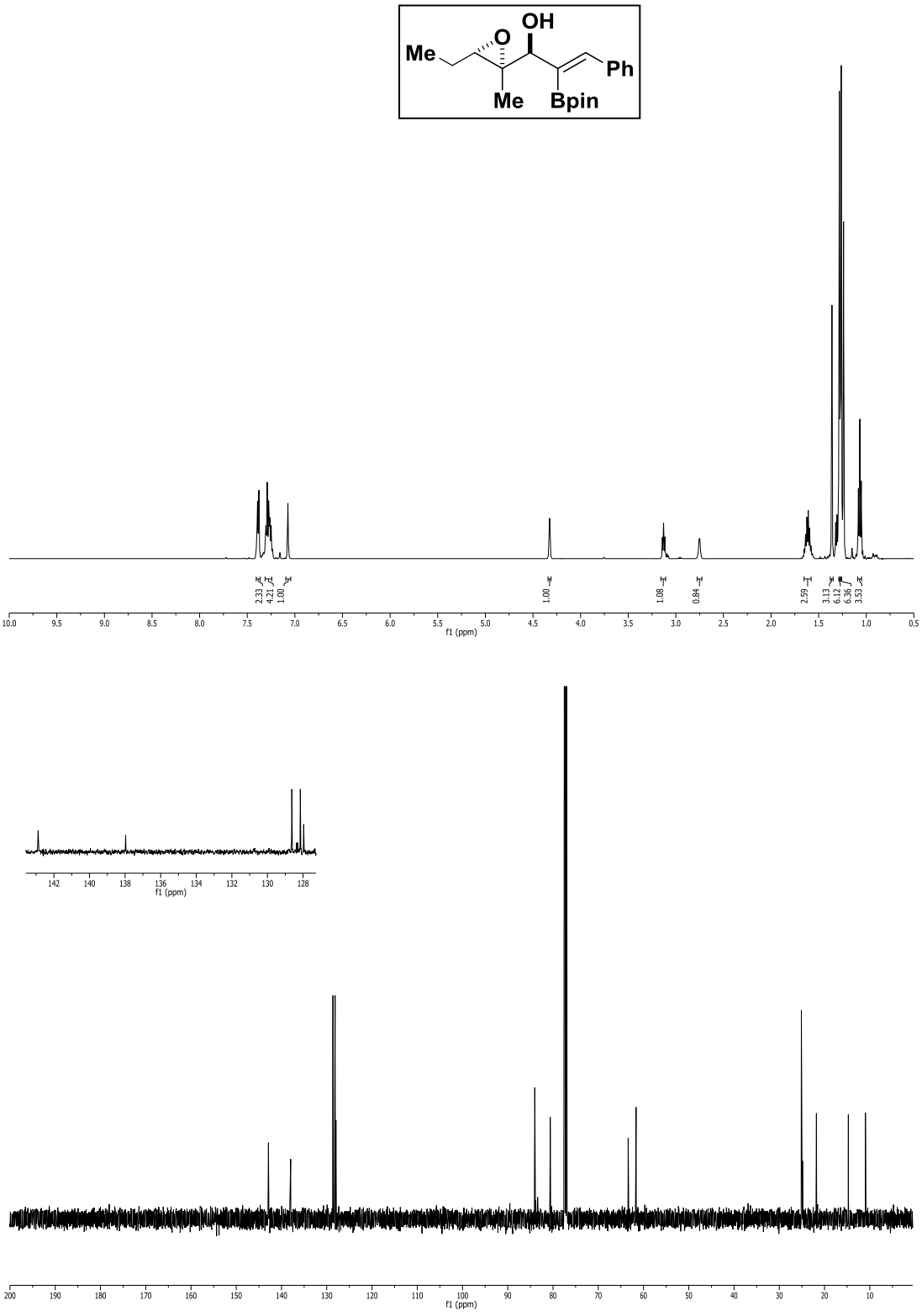

Figure S19 (3o). 500 MHz ^{1}H and 125 MHz $^{13}C\{^{1}H\}$ NMR of (*E*)-1-(3-ethyl-2-methyloxiran-2-yl)-3-phenyl-2-(4,4,5,5-tetramethyl-1,3,2-dioxaborolan-2-yl)prop-2-en-1-ol in $CDCl_3$.

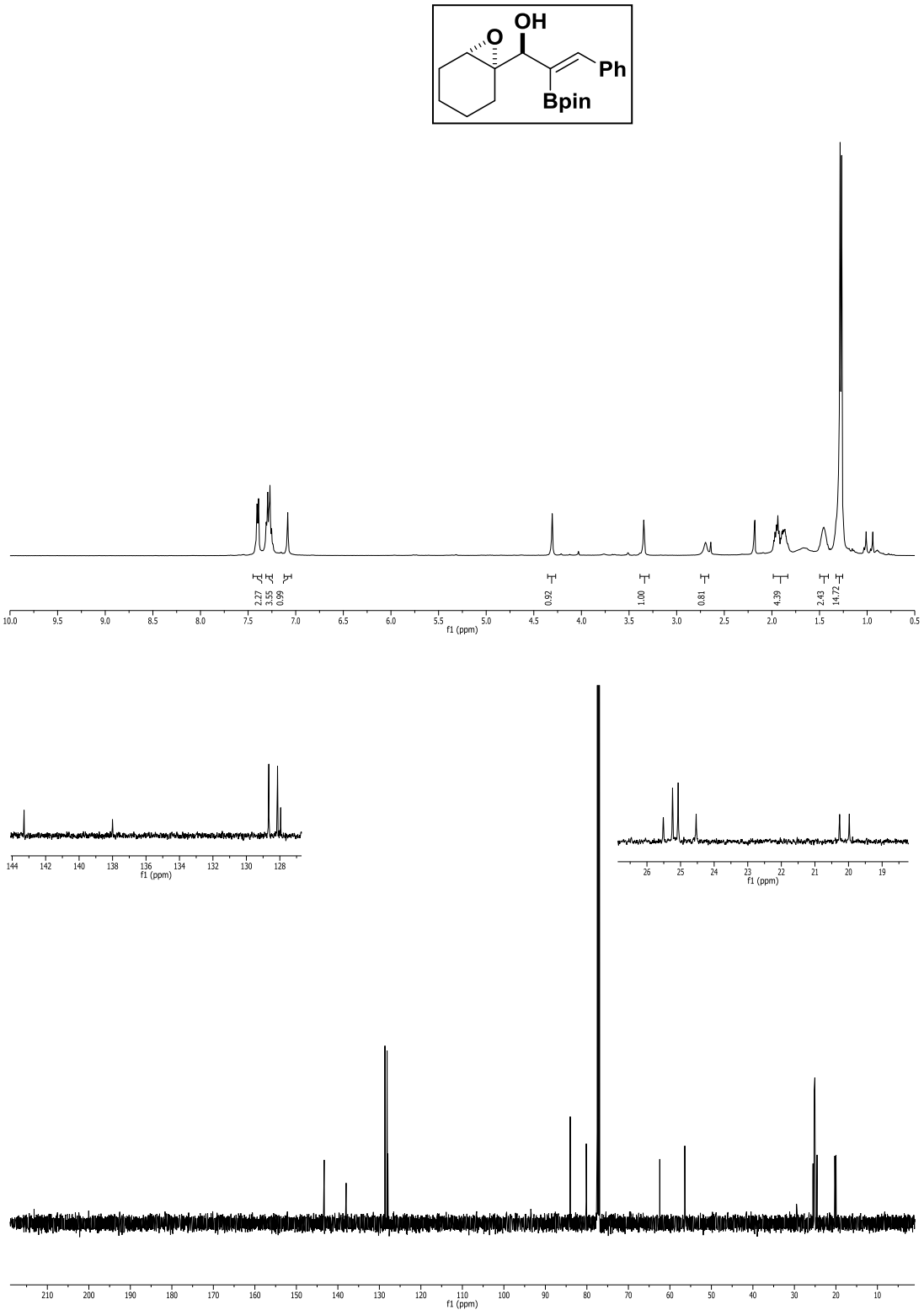

Figure S20 (3p). 500 MHz ^{1}H and 125 MHz $^{13}C\{^{1}H\}$ NMR of (*E*)-1-(7-oxabicyclo heptan-1-yl)-3-phenyl-2-(4,4,5,5-tetramethyl-1,3,2-dioxaborolan-2-yl)prop-2-en-1-ol in $CDCl_3$.

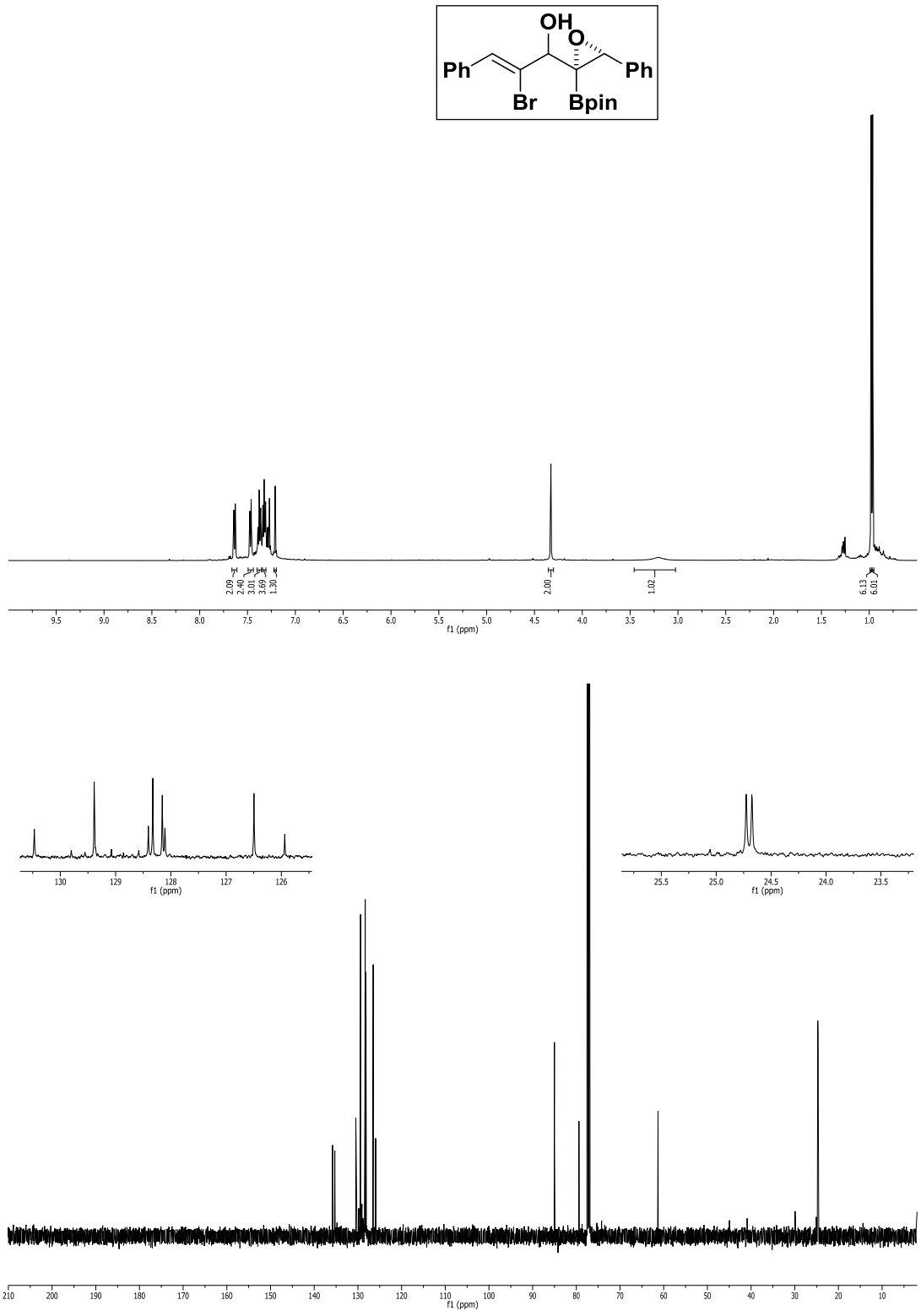

Figure S21 (4q). 500 MHz ^{1}H and 125 MHz ^{13}C{^{1}H} NMR of (*Z*)-2-bromo-3-phenyl-1-(3-phenyl-2-(4,4,5,5-tetramethyl-1,3,2-dioxaborolan-2-yl)oxiran-2-yl)prop-2-en-1-olin $CDCl_3$.

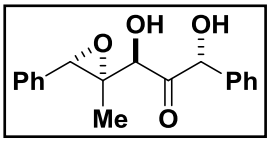

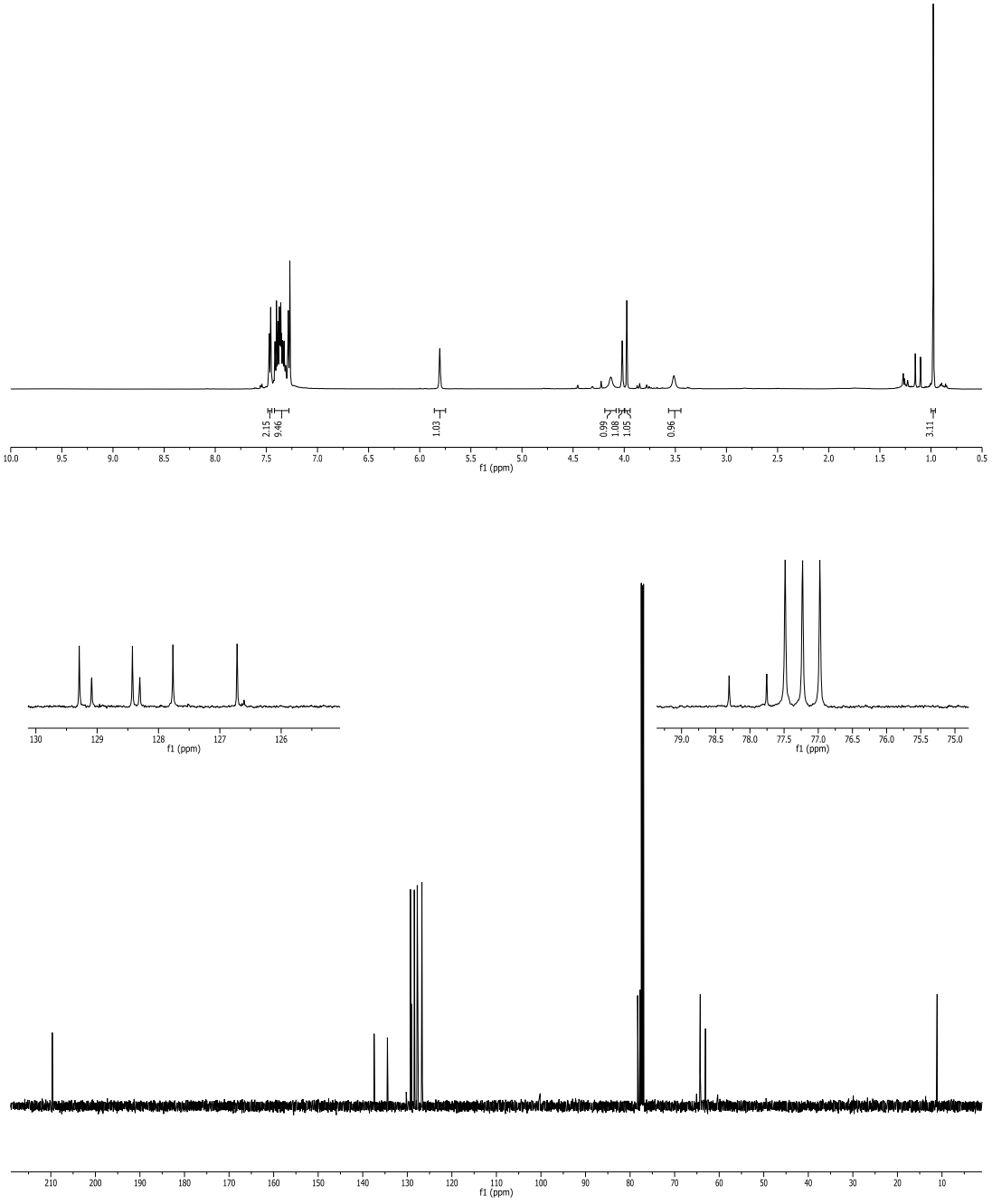

Figure S22 (5k). 500 MHz ^{1}H and 125 MHz $^{13}C\{^{1}H\}$ NMR of 1,3-dihydroxyl-1-(2-methyl-3-phenyloxiran-2-yl)-3-phenylpropan-2-one in $CDCl_3$.

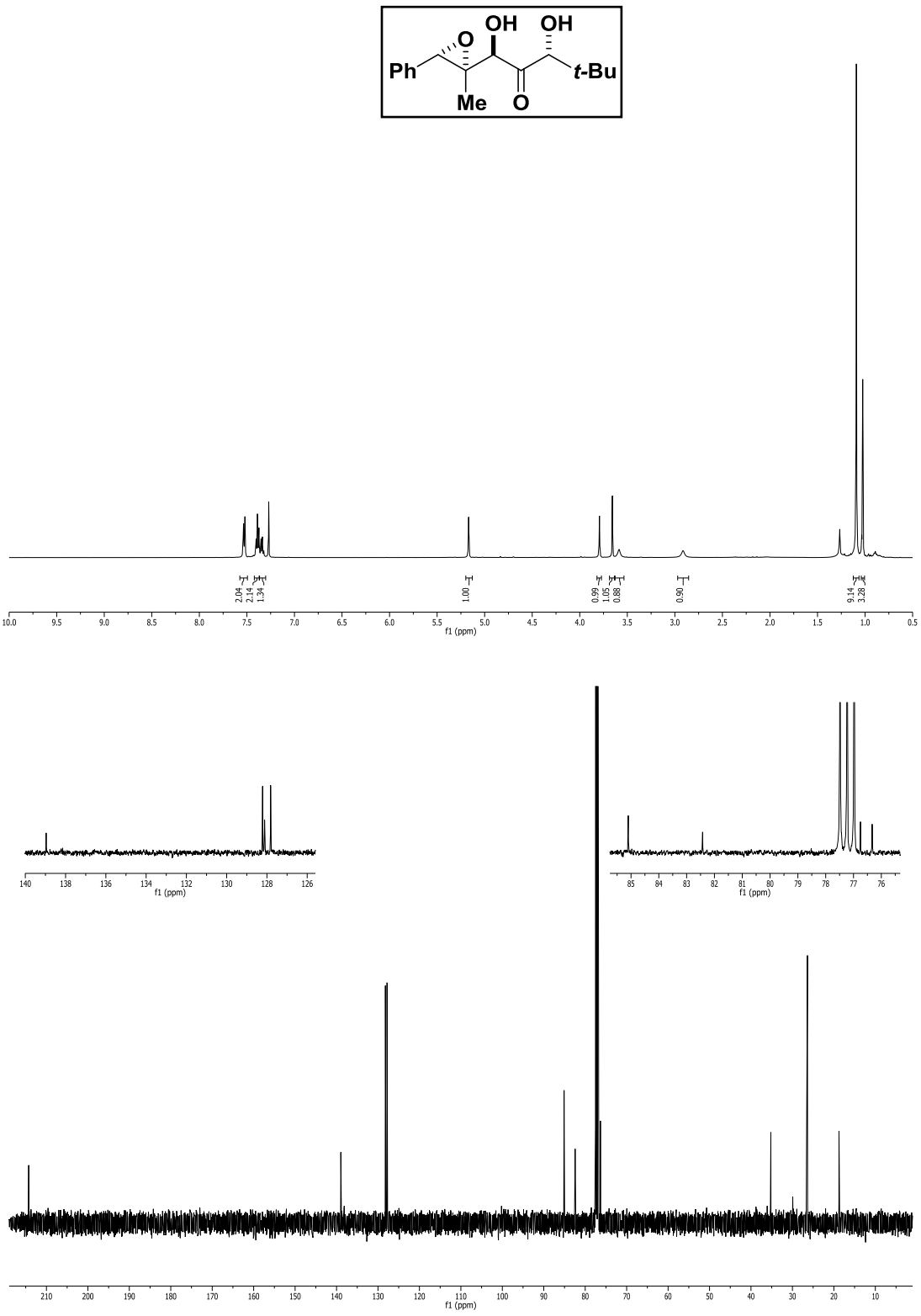

Figure S23 (5l). 500 MHz ^{1}H and 125 MHz $^{13}C\{^{1}H\}$ NMR of 1,3-dihydroxy-4,4-dimethyl-1-(2-methyl-3-phenyloxiran-2-yl)pentan-2-one in $CDCl_3$.

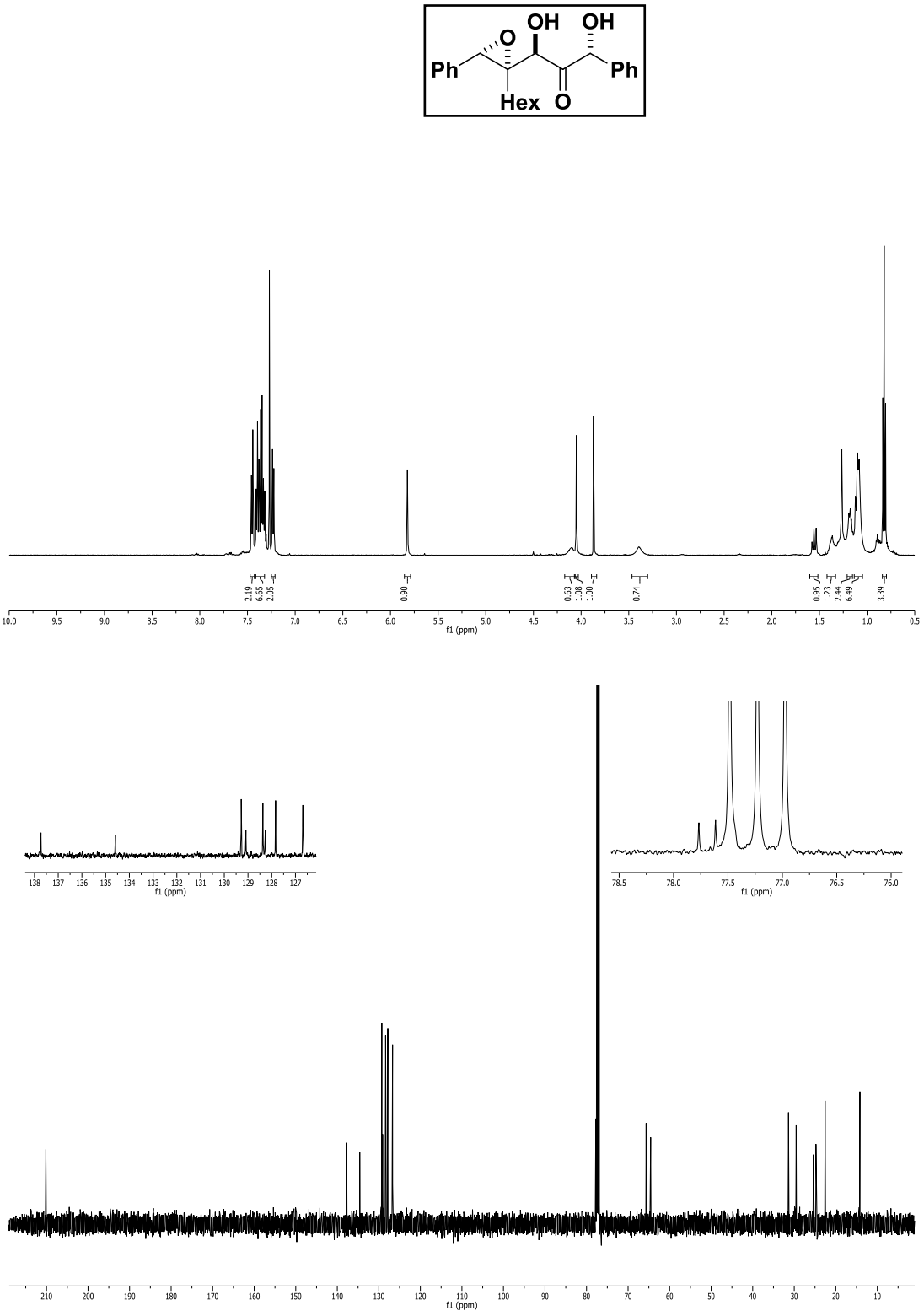

Figure S24 (5m). 500 MHz ^{1}H and 125 MHz ^{13}C{^{1}H} NMR of 1-(2-hexyl-3-phenyloxiran-2-yl)-1,3-dihydroxy-3-phenylpropan-2-one in $CDCl_3$.

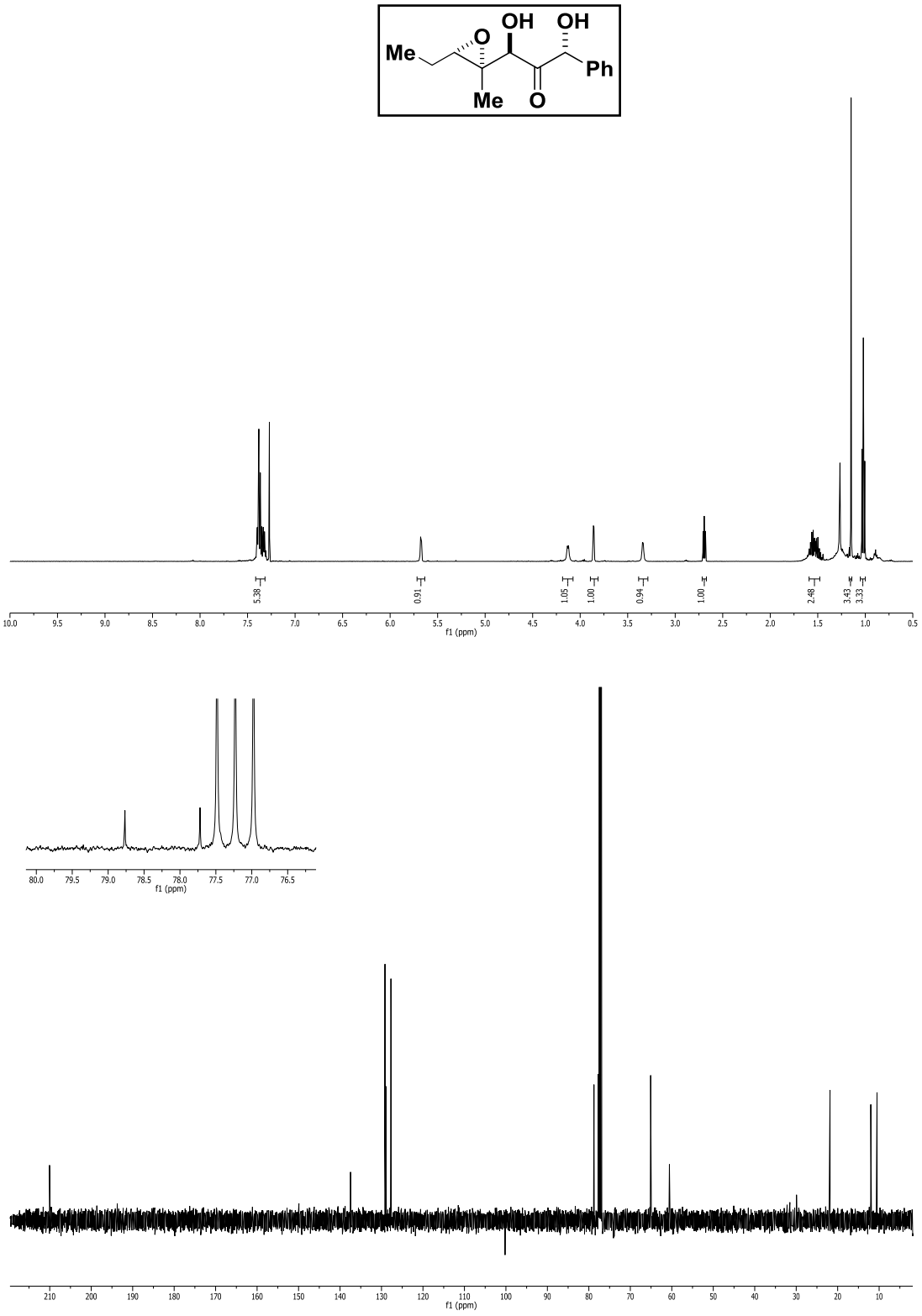

Figure S25 (5o). 500 MHz ^{1}H and 125 MHz $^{13}C\{^{1}H\}$ NMR of 1-(3-ethyl-2-methyloxiran-2-yl)-1,3-dihydroxy-3-phenylpropan-2-one in $CDCl_3$.

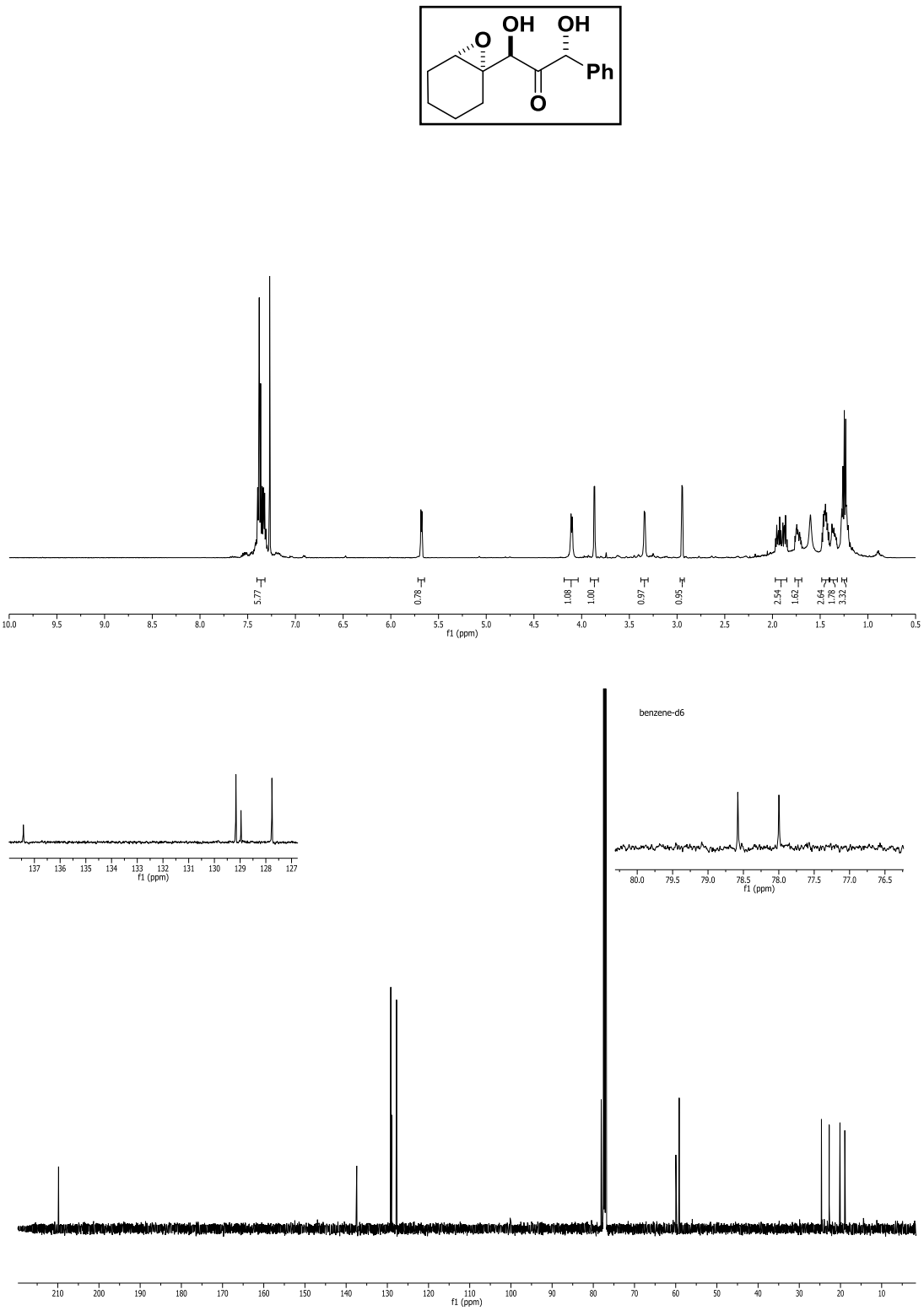

Figure S26 (5p). 500 MHz ^{1}H and 125 MHz ^{13}C{^{1}H} NMR of 1-(7-oxabicycloheptan-1-yl)-1,3-dihydroxy-3-phenylpropan-2-one in $CDCl_3$.

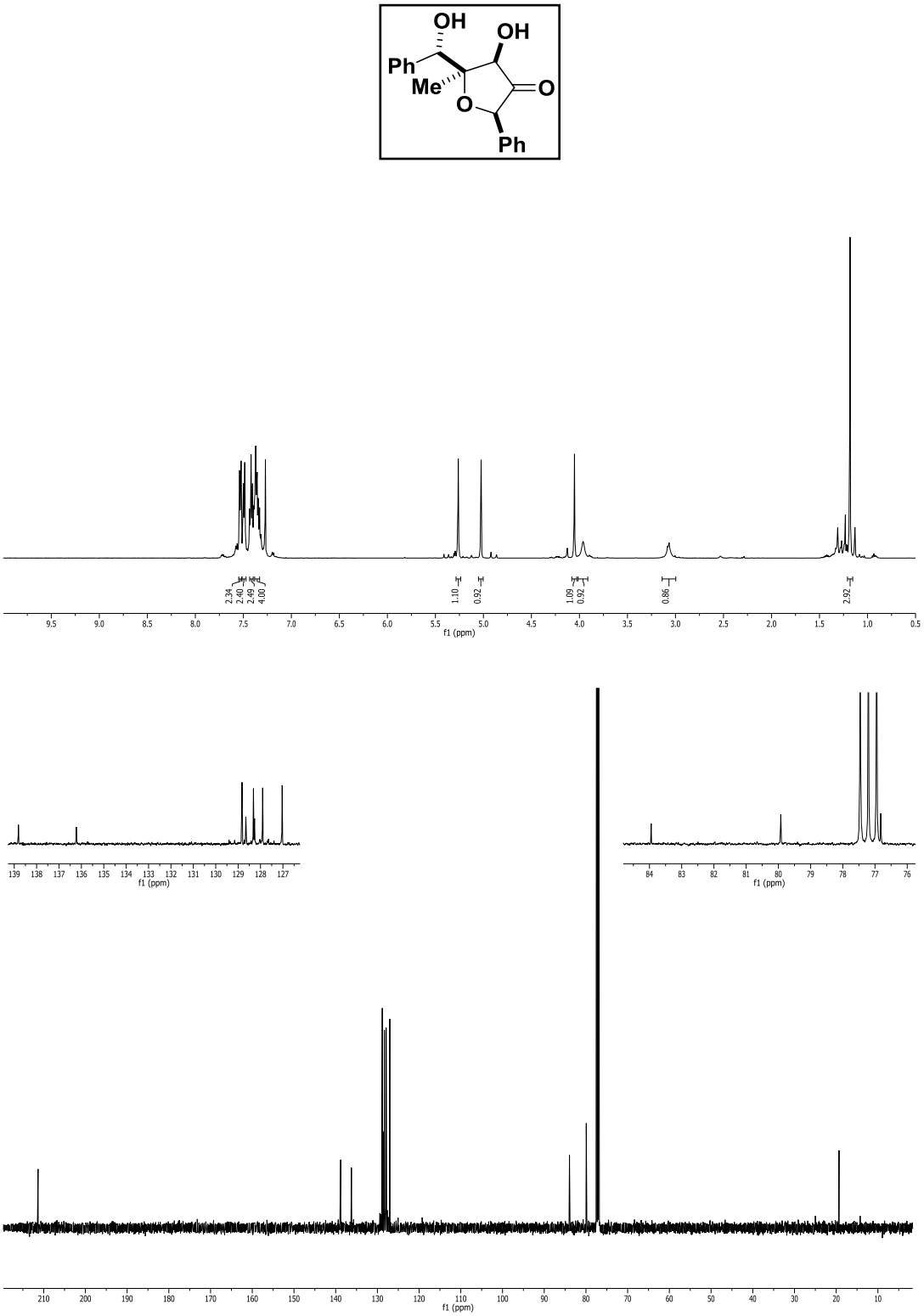

Figure S27 (6k). 500 MHz ^{1}H and 125 MHz $^{13}C\{^{1}H\}$ NMR of 4-hydroxy-5-(hydroxyl(phenyl)methyl)-5-methyl-2-phenyldihydrofuran-3-(2*H*)-one in $CDCl_3$.

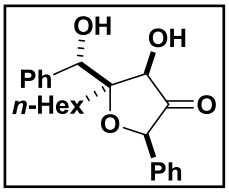

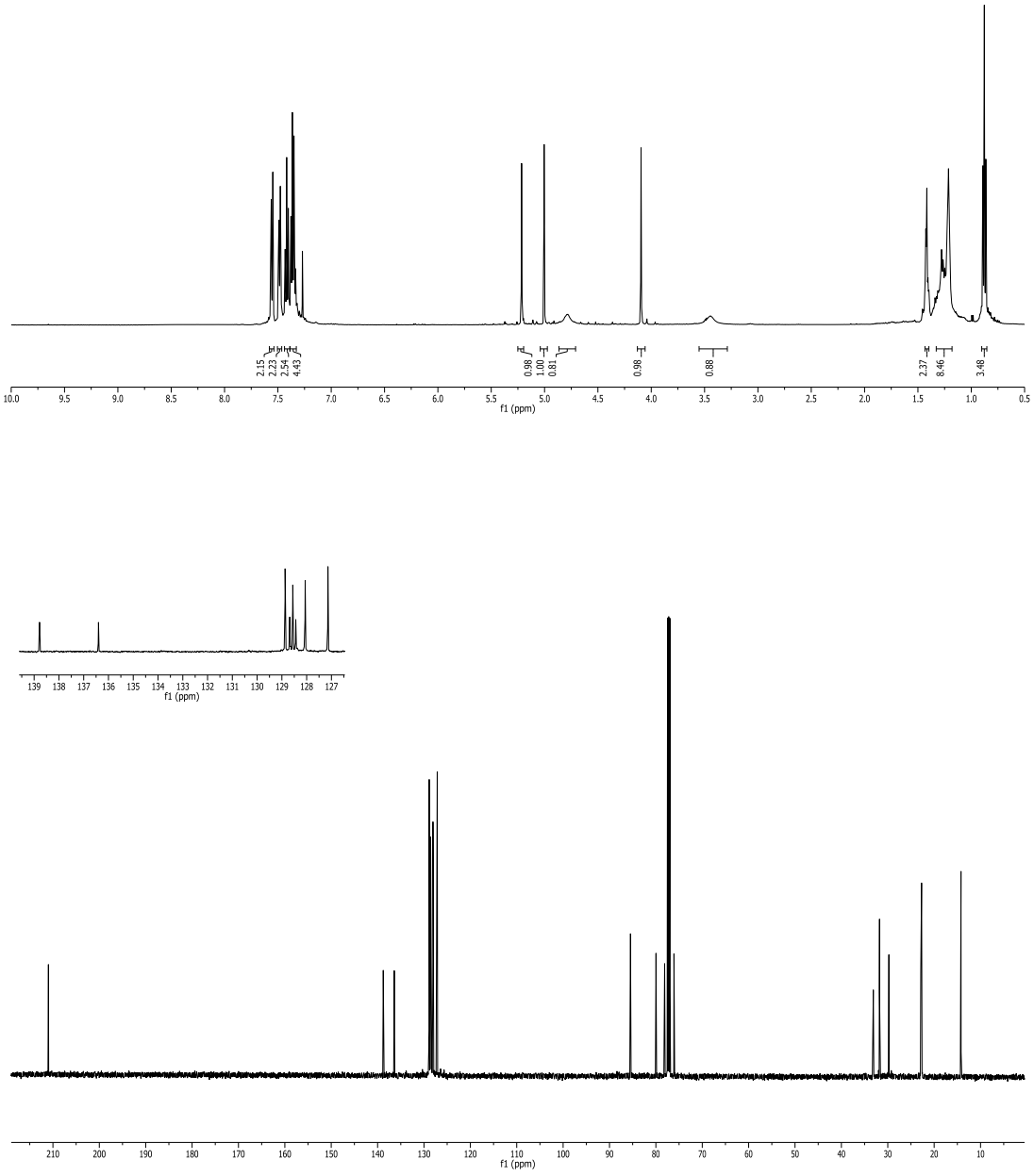

Figure S28 (6m). 500 MHz ^{1}H and 125 MHz $^{13}C\{^{1}H\}$ NMR of 5-hexyl-4-hydroxy-5-(hydroxyl(phenyl)methyl-2-phenyldihydrofuran-3-2(H)-one in $CDCl_3$.

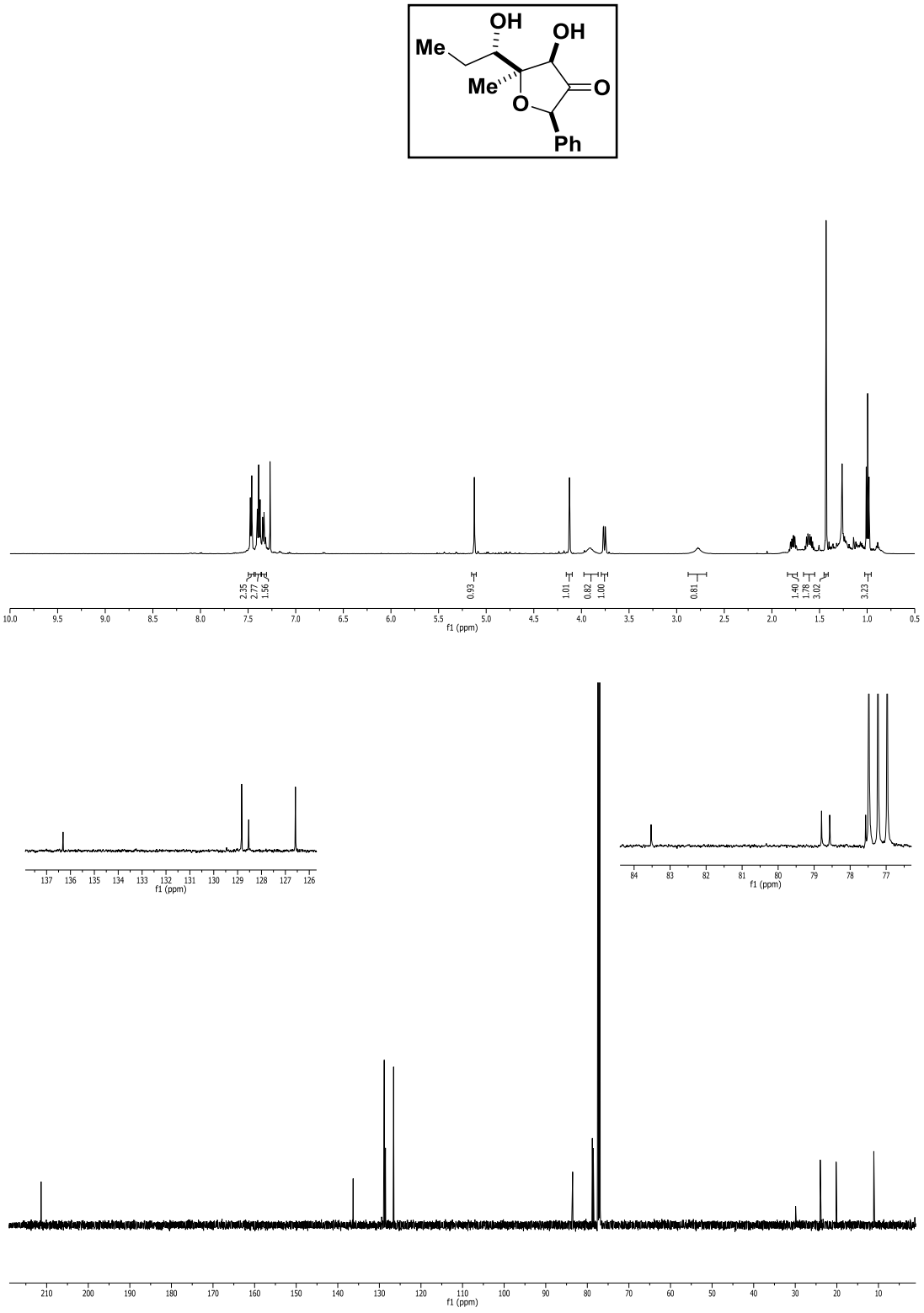

Figure S29 (6o). 500 MHz ^{1}H and 125 MHz ^{13}C{^{1}H} NMR of 4-hydroxy-5-(1-hydroxypropyl)-5-methyl-phenyldihydrofuran-3(2*H*)-one in $CDCl_3$.

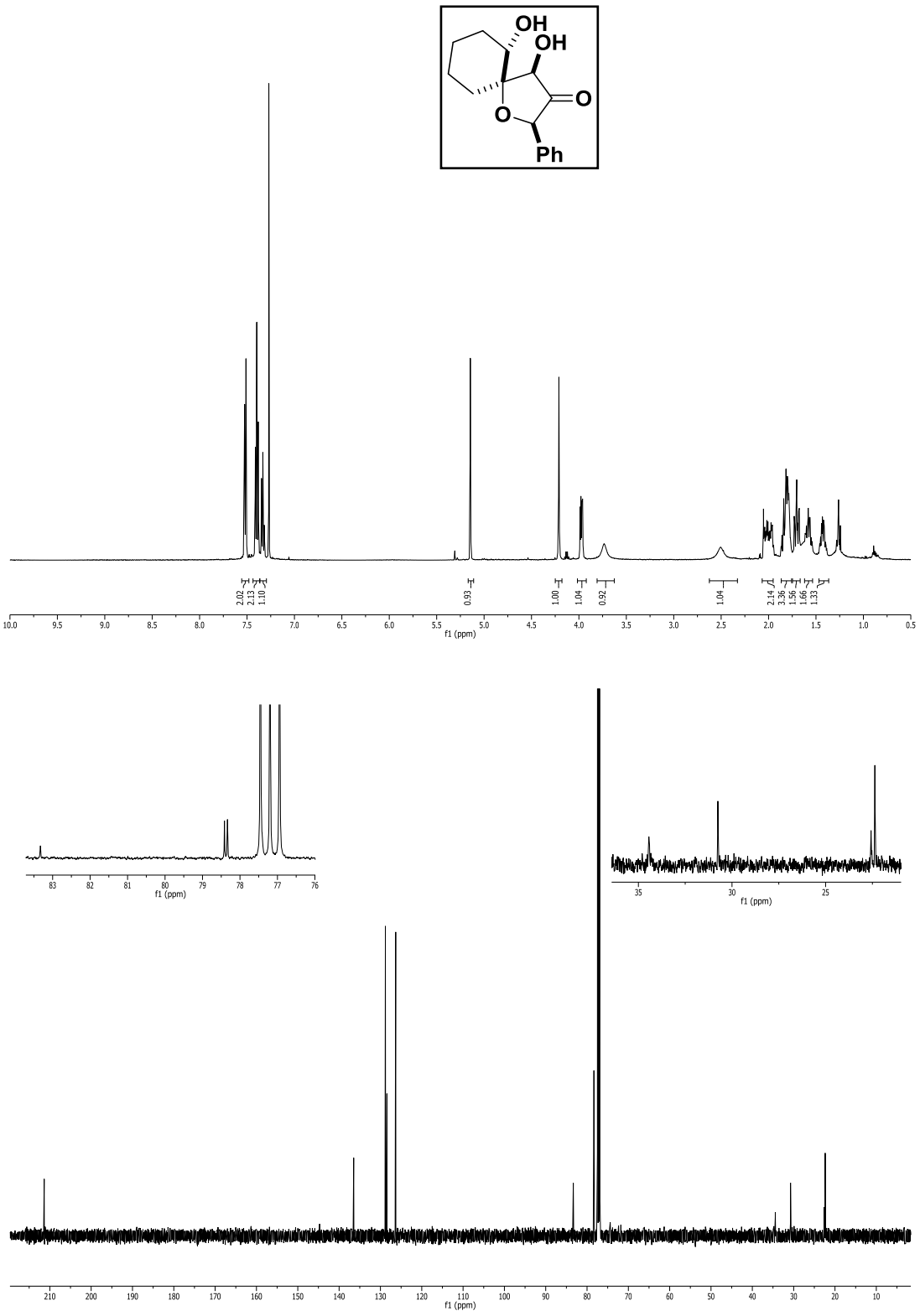

Figure S30 (6p). 500 MHz ^{1}H and 125 MHz ^{13}C{^{1}H} NMR of 4,6-dihydroxy-2-phenyl-1-oxaspiro[4,5]decan-3-one in $CDCl_3$.

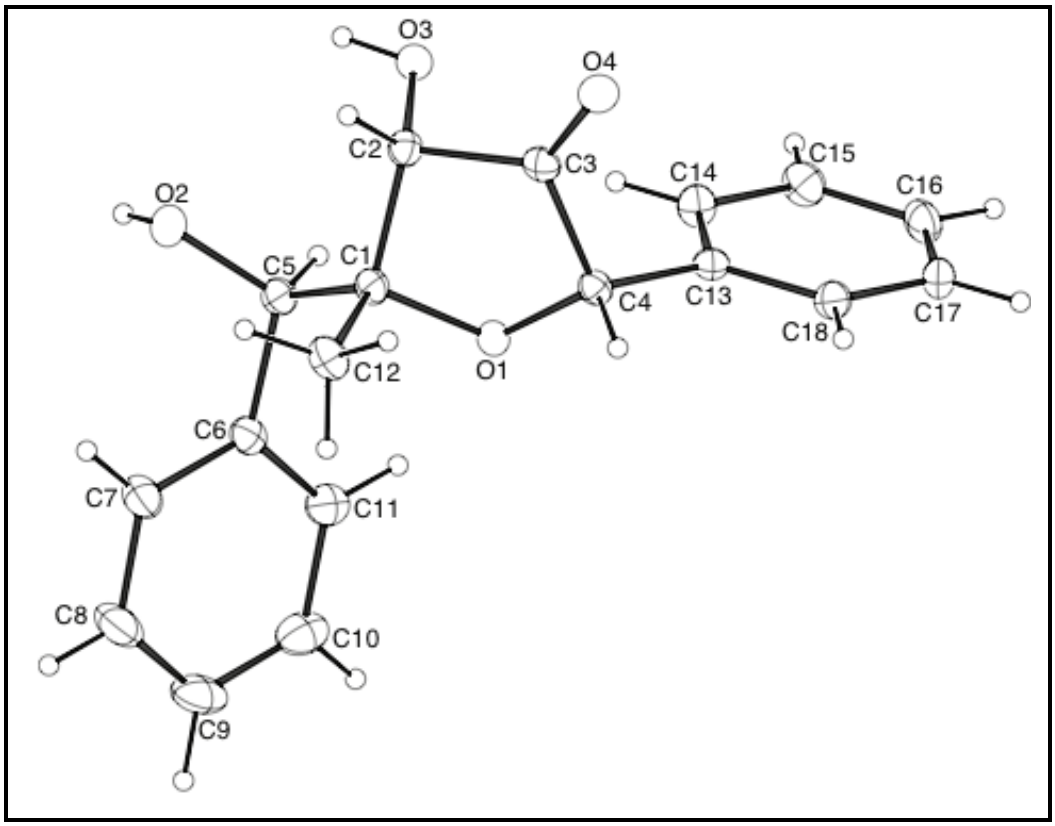

Figure S31. ORTEP drawing of 4-hydroxy-5-(hydroxyl(phenyl)methyl)-5-methyl-2-phenyldihydrofuran-3-(2*H*)-one (**6k**) with 30% probability thermal ellipsoids.

Preliminary Computational Studies:

All calculations were optimized using *GAUSSIAN09*[1], B3LYP[2-5] or M06-2X[6, 7] functional with the 6-31G(d) or 6-311G(d,p), basis set in the gas phase and in dichloromethane using CPCM[8] solvation model and UFF radii.[9-11] Optimizing transition state structures using (U)B3LYP with guess=(mix, always) did not revealed any changes in spin state. Frequency analysis was used to characterize each stationary point as minima or transition state structure. Further, IRC[12, 13] calculations were carried out on model systems to connect transition state structures to minima.

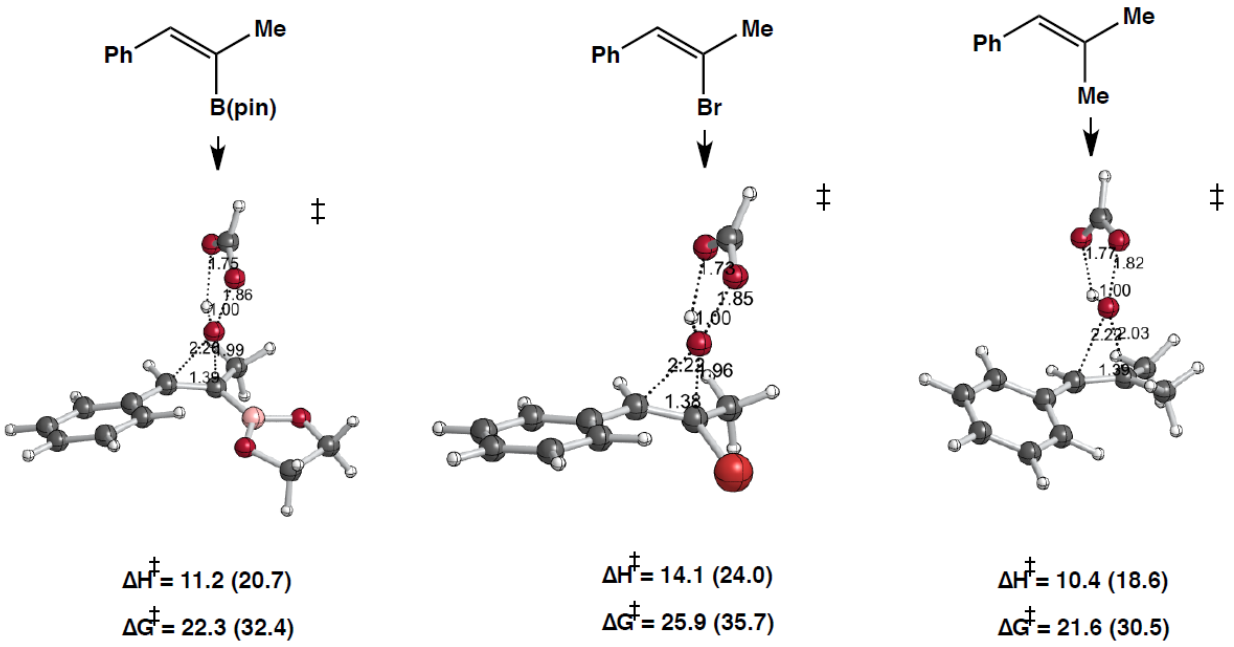

Figure S31. Relative barriers for epoxidations of model alkenes. All structures were calulated using B3LYP/6-31G(d) in gas phase and in dichloromethane (CPCM;UFF radii), in parenthesis, using M06-2X/6-311G(d,p). Reported energies are in kcal/mol. Pinacolato ligand was modeled as $C_2H_4O_2$.

References:

1. M. J. Frisch, G. W. Trucks, H. B. Schlegel, G. E. Scuseria, M. A. Robb, J. R. Cheeseman, G. Scalmani, V. Barone, B. Mennucci, G. A. Petersson, H. Nakatsuji, M. Caricato, X. Li, H. P. Hratchian, A. F. Izmaylov, J. Bloino, G. Zheng, J. L. Sonnenberg, M. Hada, M. Ehara, K. Toyota, R. Fukuda, J. Hasegawa, M. Ishida, T. Nakajima, Y. Honda, O. Kitao, H. Nakai, T. Vreven, J. A. Montgomery, J. Peralta, J. E., F. Ogliaro, M. Bearpark, J. J. Heyd, E. Brothers, K. N. Kudin, V.

N. Staroverov, R. Kobayashi, J. Normand, K. Raghavachari, A. Rendell, J. C. Burant, S. S. Iyengar, J. Tomasi, M. Cossi, N. Rega, J. M. Millam, M. Klene, J. E. Knox, J. B. Cross, V. Bakken, C. Adamo, J. Jaramillo, R. Gomperts, R. E. Stratmann, O. Yazyev, A. J. Austin, R. Cammi, C. Pomelli, J. W. Ochterski, R. L. Martin, K. Morokuma, V. G. Zakrzewski, G. A. Voth, P. Salvador, J. J. Dannenberg, S. Dapprich, A. D. Daniels, O. Farkas, J. B. Foresman, J. V. Ortiz, J. Cioslowski and D. J. Fox, *Gaussian 09, Revision A.02.*, Gaussian, Inc., Wallingford CT, 2009., 2009.

2. A. D. Becke, *J. Chem. Phys.*, 1993, **98**, 5648.
3. A. D. Becke, *J. Chem. Phys.*, 1993, **98**, 1372.
4. C. Lee, W. Yang and R. G. Parr, *Phys. Rev. B: Condens. Matter Mater. Phys.*, 1988, **37**, 785.
5. P. J. Stephens, F. J. Devlin, C. F. Chabalowski and M. J. Frish, *J. Phys. Chem.*, 1994, **98**, 11623.
6. Y. Zhao and D. G. Thrular, *Theor. Chem. Acc.*, 2008, **120**, 215.
7. Y. Zhao and D. G. Thrular, *Acc. Chem. Res.*, 2008, **41**, 157.
8. V. Barone and M. Cossi, *J. Phys. Chem. A.*, 1998, **102**, 1995.
9. D. A. Singleton, S. R. Merrigan, J. Liu and K. N. Houk, *J. Am. Chem. Soc.*, 1997, **119**, 3385.
10. K. N. Houk, J. Liu, N. C. Demello and K. R. Condroski, *J. Am Chem. Soc.*, 1997, **119**, 10147.
11. R. D. Bach, C. Canepa, J. E. Winter and P. E. Blanchette, *J. Org. Chem.*, 1997, **62**, 5191.
12. C. Gonzalez and H. B. Schlegel, *J. Phys. Chem.*, 1990, **94**, 5523.
13. K. Fukui, *Acc. Chem. Res.*, 1981, **14**, 363.